Molecular Pharmacology Fast Forward. Published on September 16, 2020 as DOI: 10.1124/molpharm.120.000047
This article has not been copyedited and formatted. The final version may differ from this version.

MOLPHARM-AR-2020-000047R2

Title: Transient Receptor Potential Ankyrin-1 (TRPA1) and Vanilloid-3 (TRPV3) Differentially Regulate Endoplasmic Reticulum Stress and Cytotoxicity in Human Lung Epithelial Cells Following Pneumotoxic Wood Smoke Particle Exposure

Authors: Nam D. Nguyen, Tosifa A. Memon, Katherine L. Burrell, Marysol Almestica-Roberts, Emmanuel Rapp, Lili Sun, Abigail F. Scott, Cassandra E. Deering-Rice, Joseph E. Rower and Christopher A. Reilly

Affiliations: (NDN, TAM, KLB, MAR, ER, LS, AFS, CEDR, JER, CAR) Department of Pharmacology and Toxicology, Center for Human Toxicology, University of Utah, 30 S 2000 E, Room 201 Skaggs Hall, Salt Lake City, Utah 84112, USA

Molecular Pharmacology Fast Forward. Published on September 16, 2020 as DOI: 10.1124/molpharm.120.000047
This article has not been copyedited and formatted. The final version may differ from this version.

MOLPHARM-AR-2020-000047R2

Running Title: TRPA1, TRPV3 and Wood Smoke Particle Toxicity

***Corresponding author:**
Dr. Christopher A. Reilly, Ph.D.
University of Utah
Department of Pharmacology and Toxicology
30 South 2000 East, 201 Skaggs Hall
Salt Lake City, UT 84112
Phone: (801) 581-5236; FAX: (801) 585-5111
Email: Chris.Reilly@pharm.utah.edu

Number of text pages: 29
Number of Tables: 1
Number of Figures: 11 (9 Figures, 2 Schemes)
References: 34
Number of words in Abstract: 205
Number of words in Introduction: 698
Number of words in Discussion: 1279

Non-Standard Abbreviations: TRPC1, transient receptor potential canonical-1, TRPA1, transient receptor potential ankyrin-1; TRPV3, transient receptor potential vanilloid-3; ATF3, activating transcription factor-3; ATF4, activating transcription factor-4; ATF6, activating transcription factor-6; IRE1, inositol requiring element-1; DDIT3, DNA damage inducible transcript-3; XBP1, X-box binding protein-1; XBP1s, spliced transcript of X-box binding protein-1; XBP1u, un-spliced transcript of X-box binding protein-1; ER, endoplasmic reticulum; ERS, endoplasmic reticulum stress, CS, cigarette smoke; WSPM, wood smoke particulate matter; BiP/ GRP78, binding immunoglobulin protein; PERK/eIF2αK3, protein kinase R-like endoplasmic reticulum kinase; HSPA1A, heat shock 70kDa protein 1; AITC, allyl isothiocyanate; DTT, dithiothreitol; BEAS-2B, human bronchial epithelial cells; HBEC, human bronchial epithelial cell; HBEC-3KT, normal human bronchial epithelial cells immortalized with CDK4 and hTERT; HEK, human embryonic kidney; SAEC, small airway epithelial cell; TRPV3OE, BEAS-2B cells stably overexpressing TRPV3; LHC-9, Lechner and LaVeck media; PBS, phosphate-buffered saline; PCR, polymerase chain reaction; qPCR, quantitative real-time PCR; β2M, beta-2 microglobulin; ANOVA, analysis of variance.

Keywords: Transient receptor potential channel, particulate matter, air pollution, lung

Molecular Pharmacology Fast Forward. Published on September 16, 2020 as DOI: 10.1124/molpharm.120.000047
This article has not been copyedited and formatted. The final version may differ from this version.

Abstract:

This study investigated the roles of Transient Receptor Potential Ankyrin-1 (TRPA1) and TRP Vanilloid-3 (TRPV3) in regulating endoplasmic reticulum stress (ERS) and cytotoxicity in human bronchial epithelial cells (HBECs) treated with pneumotoxic wood smoke particulate matter (WSPM) and chemical agonists of each channel. Functions of TRPA1 and TRPV3 in pulmonary epithelial cells remain largely undefined. This study shows that TRPA1 activity localizes to the plasma membrane and ER of cells, whereas TRPV3 resides primarily in the ER. Additionally, treatment of cells using moderately cytotoxic concentrations of pine WSPM, carvacrol, and other TRPA1 agonists, caused ERS as a function of both TRPA1 and TRPV3 activities. Specifically, ERS and cytotoxicity were attenuated by TRPA1 inhibition, while inhibiting TRPV3 exacerbated ERS and cytotoxicity. Interestingly, following treatment with pine WSPM, TRPA1 transcription was suppressed, while TRPV3 was increased. TRPV3 overexpression in HBECs conferred resistance to ERS and an attenuation of ERS-associated cell cycle arrest caused by WSPM and multiple prototypical ERS-inducing agents. Alternatively, shRNA-mediated knockdown of TRPV3, like the TRPV3 antagonist, exacerbated ERS. This study reveals previously undocumented roles for TRPA1 in promoting pathological ERS and cytotoxicity elicited by pneumotoxic WSPM and TRPA1 agonists, and a unique role for TRPV3 in fettering pathological facets of the integrated ERS response.

Significance Statement: These findings provide new insights into how WSPM and other TRPA1 and TRPV3 agonists can affect HBECs, and highlight novel physiological and pathophysiological roles for TRPA1 and TRPV3 in these cells.

Molecular Pharmacology Fast Forward. Published on September 16, 2020 as DOI: 10.1124/molpharm.120.000047
This article has not been copyedited and formatted. The final version may differ from this version.

Introduction:

Wood/biomass smoke and particulate emissions (WSPM) are a major human health risk. Exposure to high concentrations of particulate material (PM) from multiple types of wood and biomass has been linked to increased rates of hospital admissions for respiratory complications due to acute lung inflammation, tissue damage, and respiratory distress (Swiston *et al.*, 2008; Ghio *et al.*, 2012; Reid *et al.*, 2016; Liu *et al.*, 2017). Long-term exposure is also associated with the development and exacerbation of chronic diseases including asthma, emphysema, and chronic obstructive pulmonary disease (Laumbach and Kipen, 2012; Olloquequi and Silva, 2016). Currently, mechanisms by which WSPM affect the respiratory tract are not fully understood.

WSPM is a complex mixture of solids and condensed chemicals with variable pneumotoxic potential (Kim *et al.*, 2018). Our laboratory has shown that WSPM from pine, mesquite, and other fuels differentially activate the TRPA1 and TRPV3 ion channels (Shapiro *et al.*, 2013; Deering-Rice *et al.*, 2018). Neuronal TRPA1 is a mediator of pulmonary irritation and inflammation (Andrè *et al.*, 2008; Bessac *et al.*, 2008), but the functions of TRPA1 in non-neuronal cells are less understood. Studies have shown that pine and other forms of WSPM, pure TRPA1 agonists (i.e., AITC and coniferaldehyde), as well as diesel exhaust particles (DEP), stimulate the expression and secretion of gel-forming mucins (MUC5AC and 5B), as well as MUC4, by activating TRPA1 in primary human bronchial epithelial cells (HBECs) (Deering-Rice *et al.*, 2019; Memon *et al.*, 2020). Consequences of TRPV3 activation in HBECs by WSPM have also been explored (Deering-Rice *et al.*, 2018). For example, TRPV3 overexpression in BEAS-2B lung cells (TRPV3OE cells) was found to increase the cytotoxicity of pine WSPM and TRPV3 inhibition reduced the cytotoxicity. Additionally, a TRPV3 antagonist prevented changes in pulmonary function associated with sub-chronic pine WSPM treatment in mice. However, detailed

Molecular Pharmacology Fast Forward. Published on September 16, 2020 as DOI: 10.1124/molpharm.120.000047
This article has not been copyedited and formatted. The final version may differ from this version.

mechanisms for how TRPA1 and TRPV3 ultimately influenced the cytotoxicity of WSPM were not defined, leaving critical knowledge gaps surrounding the physiological and pathophysiological functions of these channels in airway epithelial cells.

Our laboratory previously demonstrated that activation of TRPV1 in HBEC cells using cell-permeable agonists caused lung epithelial cell death through disruption of endoplasmic reticulum (ER) calcium homeostasis and initiation of pathological ER stress (ERS) (Thomas *et al.*, 2011, 2012). ERS is a conserved collection of processes that become activated when protein-folding and/or secretion are disrupted (Korfei *et al.*, 2016), as outlined by Scheme 1. ERS has been linked to various lung pathologies including mucus hypersecretion in individuals with asthma and cystic fibrosis, due to ectopic inositol requiring element-1 (IRE1)-β activity (Martino *et al.*, 2013). IRE1 is a key regulatory element of the integrated ERS response and is generally considered to be central in the coordination of adaptive responses during stress. Additionally, a role for the ERS-regulated gene DNA Damage Inducible Transcript-3 (DDIT3) has been shown in idiopathic pulmonary fibrosis (Yao *et al.*, 2016), and a role for ERS was shown in a model of cigarette smoke (CS)-induced pulmonary inflammation and emphysema (Wang *et al.*, 2017).

An array of stimuli can induce ERS and include oxidative stress, misfolding of proteins due to mutations or chemical modification, viral infection, glucose starvation, as well as calcium store depletion, including through the activation of TRP channels (Xu *et al.*, 2005; Thomas *et al.*, 2012). While several studies have shown that ERS can also occur in HBECs and in lungs exposed to PM (Watterson *et al.*, 2009; Xu *et al.*, 2019), a role of TRPA1 in regulating ERS and the roles of TRPA1 and ERS in WSPM toxicity have not been explored. It is also currently unknown whether TRPV3 can regulate ERS and/or cytotoxicity in HBECs as a result of stimulation by WSPM or other toxins.

Molecular Pharmacology Fast Forward. Published on September 16, 2020 as DOI: 10.1124/molpharm.120.000047
This article has not been copyedited and formatted. The final version may differ from this version.

The hypothesis of this study was that pine WSPM, as well as TRPA1 and TRPV3 agonists would promote HBEC cytotoxicity through activation of TRPA1 and/or TRPV3, ER calcium depletion, and initiation of pathological ERS. The objectives of this study were: 1) to delineate mechanisms by which pneumotoxic WSPM affect HBEC viability; and 2) to elucidate roles for TRPA1 and TRPV3 in regulating cytotoxicity caused by a model pneumotoxic pollutant, pine WSPM, and prototypical TRPA1 and TRPV3 agonists that mimic the effects of WSPM on these channels.

Materials and Methods:

Chemicals: All chemicals were purchased from Cayman Chemical or Sigma-Aldrich unless otherwise specified. A TRPV3 antagonist previously described by Hydra Biosciences: 2-(5-trifluoromethyl-pyridine-2-ylsulfanyl)-1-(8-methyl-3,4-dihydro-2H-quinolin-1-yl)-ethanone, was synthesized as previously described (Deering-Rice *et al.*, 2014). For simplicity and consistency with our prior studies, we refer to this molecule as simply "TRPV3 antagonist."

Size-fractionated pine WSPM and other forms of WSPM (i.e., juniper, apple wood, range grass, Colorado sage, goat, sheep and cow dung smoke PM) were prepared using a laboratory furnace as previously described (Shapiro *et al.*, 2013). Juniper and Colorado sage were collected in the fall season near the four corners region of Colorado. Apple wood was from tree trimmings of a mature tree grown in Salt Lake City, UT and range grass was collected from the Salt Lake City foothills, also in the fall. Animal dung was collected fresh in a clean room facility from animals housed at the USDA Agricultural Research Services facility (Logan, UT), from animals maintained on standard diets. The feces samples were dried at room temperature in a fume hood over multiple days. For all experiments, with the exception of results in Supplemental Figures 1

Molecular Pharmacology Fast Forward. Published on September 16, 2020 as DOI: 10.1124/molpharm.120.000047
This article has not been copyedited and formatted. The final version may differ from this version.

and 4 (Supp. Figs. 1 and 4), fraction 7 (0.43-0.65 μm) WSPM was used. In all cases, WSPM was solubilized in DMSO at a stock concentration of 115 mg/mL and diluted into media as needed, with the DMSO content at 2% or less. Because WSPM is unstable when stored and after resuspension for experiments, materials were not used beyond 3 months post-production date and were prepared fresh for each experiment. Further, the potency of each batch of WSPM was verified for potency in TRPA1 and TRPV3 calcium flux assays, and must fall within a consistent range that we have determined empirically to be an average and to produce a consistent range of results in our various endpoint assays.

Cell Culture: Cells were maintained at 37ºC and 5% CO_2 in a humidified incubator. TRP channel-overexpressing HEK-293 cells were generated as previously described and cultured in DMEM:F12 medium supplemented with 5% fetal bovine serum, 1X penicillin/streptomycin, and 300 μg/mL geneticin (Deering-Rice *et al.*, 2012). BEAS-2B HBECs (ATCC; Manassas, VA) were cultured in LHC-9 medium (Life Technologies; Carlsbad, CA), and TRPV3-overexpressing BEAS-2Bs (TRPV3OE) were selected and cultured as previously described (Deering-Rice *et al.*, 2018). Primary human lobar bronchial epithelial cells (lobar HBECs; donor ID: 01344) and human small airway epithelial cells (SAECs; donor ID: 00656) were purchased from Lifeline Cell Technology (Frederick, MD). Normal human bronchial epithelial cells immortalized with CDK4 and hTERT (HBEC3-KTs) were purchased from ATCC (Manassas, VA). HBEC and SAECs were cultured using the BronchiaLife epithelial airway medium complete kit from Lifeline Cell Technology. HBEC3-KTs were cultured with airway epithelial cell basal medium supplemented with the bronchial epithelial cell growth kit from ATCC. The vehicle used for mRNA expression, western blot, cytotoxicity, and flow cytometry studies was fresh media, either fresh LHC-9 for BEAS-2B cells or BronchiaLife epithelial airway medium for lobar HBECs. Note: The lobar

Molecular Pharmacology Fast Forward. Published on September 16, 2020 as DOI: 10.1124/molpharm.120.000047
This article has not been copyedited and formatted. The final version may differ from this version.

HBEC, SAEC, and HBEC-3KT cells used in this study all have the TRPV1 I585I/V (rs8065080) genotype, which has previously been shown to correlate with higher levels of TRPA1 expression (Deering-Rice *et al.*, 2016). Alternatively, the BEAS-2B cells and derivative lines thereof have the I585I/I genotype and consequently lower levels of TRPA1 expression. All of the cells used in this study were also homozygous wild-type for the TRPA1 R3C and R58T polymorphisms, rs13268757 and rs16937976, respectively, which have also been associated with a gain-of-function for some particle agonists and increased risk for poor asthma control (Deering-Rice *et al.*, 2015). As such, the TRPV1 and TRA1 genotypes should be considered as a variable in future studies of TRPA1 agonists on HBECs because the genotype could affect how the cells respond to various forms of PM and TRPA1 agonists. Genotyping of the cells was performed as previously described (Deering-Rice *et al.*, 2015, 2016). Finally, it was observed that the expression of TRPA1 decreased in primary cells with passaging. As such, to minimize experimental variability due to changes in basal levels of TRPA1 and TRPV3 expression, the primary HBECs were used for a maximum of 5 passages following receipt from the supplier.

Calcium Flux Assays: Pine WSPM- and TRP agonist-induced calcium flux was measured using the Fluo-4 Direct assay kit (Invitrogen; Carlsbad, CA). Calcium flux was imaged on an EVOS FL Auto microscope (ThermoFisher; Waltham, MA) as previously described (Deering-Rice *et al.*, 2011, 2012). Briefly, cells were imaged at 10X magnification using GFP filter set. Cells were maintained at room temperature (~22-23^{o}C) and agonist treatments were added to cells at 3X concentration in LHC-9, which contains 111.1 μM calcium. Images were captured every 20 seconds for 100 seconds. Changes in fluorescence were determined using an Image-J-based program and the values were corrected by subtracting the baseline fluorescence and normalized to the maximum fluorescence intensity elicited by ionomycin (10 μM), applied after agonist

Molecular Pharmacology Fast Forward. Published on September 16, 2020 as DOI: 10.1124/molpharm.120.000047
This article has not been copyedited and formatted. The final version may differ from this version.

treatment. In calcium flux experiments where thapsigargin (2.5 μM) was used as a pretreatment to deplete ER calcium stores, a transient increase in cealcium occurred. Accordingly, agonists were applied only after the intensity returned to baseline, approximately 5 minutes after thapsigargin application.

*Cytotoxicity Assay*s: For cytotoxicity assays, lobar HBEC cells were cultured in a 96-well plate at a density of 25,000 cells per well for 24h. After 24 hours, cells were then treated with pine WSPM suspended in culture media at increasing concentrations for an additional 24h. When the effects of TRPA1 and TRPV3 antagonists were tested, pine PM was applied at a fixed concentration of 20 μg/cm^2. After treatment, residual viability was measured using the Dojindo Cell Counting Kit-8 (Dojindo; Rockville, MD) according to the manufacturer protocol.

Immunocytochemical Localization of TRPV3 in HBECs: Lobar HBECs were grown on either ethanol and flame-sterilized coverslips or 8-well chamber slides, which were coated with LHC basal medium fortified with collagen (30 μg/mL), fibronectin (10 μg/mL), and bovine serum albumin fraction V (100 μg/mL). Cells were then fixed with 4% paraformaldehyde and permeabilized with 0.2% Triton X-100. Nonspecific antibody binding was blocked by incubating cells in 10% normal goat serum for 1h at room temperature (~22ºC). Cells were then incubated with a mouse monoclonal primary antibody for TRPV3 (1:200; 73-043; Neuromab; Davis, CA) and a rabbit polyclonal primary antibody for the ER biomarker calnexin (1:1000; ab22595; Abcam; Cambridge, MA) overnight at 4ºC, followed by incubation with a goat-anti-mouse secondary antibody conjugated with AlexaFluor488 (1:1000, A-11001, Invitrogen; Carlsbad, CA) and a goat-anti-rabbit secondary antibody conjugated with AlexaFluor594 (1:1000, A-11012, Invitrogen; Carlsbad, CA). After incubation with the antibodies, cell nuclei were stained with Hoechst 33342, and cells were post-fixed with 4% paraformaldehyde. Coverslips were then mounted to microscope

Molecular Pharmacology Fast Forward. Published on September 16, 2020 as DOI: 10.1124/molpharm.120.000047
This article has not been copyedited and formatted. The final version may differ from this version.

slides with Prolong Gold Antifade Mounting Medium (Invitrogen; Carlsbad, CA). Cells were imaged on a Nikon A1R confocal microscope with a 60X oil immersion lens. TRPV3 primary antibody specificity was previously determined by western blot (Deering-Rice *et al.*, 2018). Additionally, use of this antibody for immunocytochemistry was validated by comparing naïve and TRPV3-overexpressing BEAS-2B HBECs, where staining intensity was far greater in the over-expressing cells (Supp. Fig. 3B).

qPCR Gene Expression Analysis: Cells were grown to confluence in 12-well plates. After treatment, total RNA was isolated using the PureLink RNA Mini Kit (Invitrogen; Carlsbad, CA). Total RNA (2 μg) cDNA was synthesized using the ABI High Capacity cDNA Synthesis Kit with RNase Inhibitor (Applied Biosystems; Foster City, CA). The cDNA was then subjected to analysis by qPCR using a Life Technologies QuantStudio 6 Flex instrument. Taqman probe-based assays were used for human TRPV3 (Hs00376854_m1), human TRPA1 (Hs00175798_m1), human ATF3 (Hs00231069_m1), human DDIT3 (Hs00358796_g1), and human HSPA1A (Hs00359163_s1). Fluorescent probes and primers to distinguish between the spliced (XBP1s) and un-spliced (XBP1u) transcripts of XBP1 were designed, as described elsewhere (Maiuolo *et al.*, 2011). For both XBP1s and XBP1u, the same external primers were used, each at a final concentration of 900 nM (forward primer: 5'-AAT GAA GTG AGG CCA GTG GC-3'; reverse primer: 5'TGA AGA GTC AAT ACC GCC AGA A-3'). For XBP1s, the internal probe sequence was designed to span the splice junction between exons 4 and 5 (probe sequence: 5'-TGC TGA GTC CGC AGC AGG TGC A-3'), where for XBP1u, the internal probe sequence spanned intron 4 (probe sequence: 5'-CAG CAC TCA GAC TAC GTG-3'). XBP1 probes were FAM-labeled at the 5'-end, BHQ1-labeled at the 3'-end, and used at a final concentration of 250 nM. Relative gene expression data were normalized against the housekeeping gene β2-microglobulin (β2M;

Molecular Pharmacology Fast Forward. Published on September 16, 2020 as DOI: 10.1124/molpharm.120.000047
This article has not been copyedited and formatted. The final version may differ from this version.

Hs00984230_m1) using the ΔΔCT method. The absolute number of copies of TRPA1 and TRPV3 mRNA in cells was determined using standard curves for TRPA1, TRPV3 and β2M.

Western Blot Analysis: Cells were grown to confluence in 25 cm^2 flasks. Following treatment, total protein was harvested on ice using radioimmunoprecipitation (RIPA) buffer, supplemented with 6M urea, 1% sodium dodecyl sulfate (SDS), and Halt protease inhibitor (Invitrogen; Carlsbad, CA). Lysates were sonicated on ice 3X for 3 seconds and clarified by centrifugation at 13,000×g for 15 minutes at 4ºC. Protein concentrations were determined using the bicinchoninic acid method (ThermoFisher; Waltham, MA). 30 μg of protein was loaded into each well of a 4-12% Bolt Bis-Tris 12-well gel (Invitrogen; Carlsbad, CA) and resolved by electrophoresis for 1h at 150V. Protein was transferred to a polyvinylidene fluoride (PVDF) membrane using the iBlot 2 Gel Transfer Device (Life Technologies; Carlsbad, CA). Following transfer, the membrane was blocked in SuperBlock (Invitrogen; Carlsbad, CA) for 1h at room temperature. Primary mouse monoclonal antibodies against DDIT3 (2895; Cell Signaling Technology; Danvers, MA; 1:1000 in 5% bovine serum albumin with 0.1% sodium azide) and Hsp70 (ab2787; Abcam; Cambridge, MA; 1:1000 in 5% bovine serum albumin with 0.1% sodium azide) were incubated at 4ºC overnight and used in conjunction with horse radish peroxidase-conjugated sheep-anti-mouse secondary antibodies (GE Health Sciences; Marlborough, MA; 1:10,000 in SuperBlock). SuperSignal West Dura Extended Duration Substrate was added to the membrane, and immunostaining was visualized using autoradiography film. Bands were quantified using densitometry on ImageJ, normalized against the vehicle control.

Flow Cytometry/Cell Cycle Analysis: BEAS-2B and TRPV3OE cells were grown to ~50% confluence, treated for 4h, collected by trypsinization, and fixed in 66% ice-cold ethanol. Following fixation, cell nuclei were stained and analyzed using the Propidium Iodide Flow

Molecular Pharmacology Fast Forward. Published on September 16, 2020 as DOI: 10.1124/molpharm.120.000047
This article has not been copyedited and formatted. The final version may differ from this version.

Cytometry Kit (ab139418; Abcam; Cambridge, MA) according to manufacturer specifications. Analysis of samples was performed at the University of Utah Flow Cytometry Core facility using the BD FACS Canto Analyzer. A sublethal dose of pine WSPM (5 μg/cm^2) was used for cell cycle analysis experiments to minimize cell damage and death while still capturing cell cycle arrest.

Knockdown of TRPV3 in BEAS-2B HBECs: BEAS-2B cells were transfected with 1 μg TRPV3-specific construct D or control/scrambled shRNA plasmid DNA provided with the TRPV3 Human shRNA Plasmid Kit (Locus ID: 162514; TF300805; OriGene Technologies, Rockville, MD) using FUGENE 6 transfection reagent (3:1 reagent to DNA). Stable overexpression of the shRNA construct was selected using resistance to puromycin (1 μg/mL) and RFP-overexpression. Puromycin resistant and RFP-positive colonies were subsequently isolated, expanded, and screened for knockdown of TRPV3 by qPCR and functional assays. A single colony showing changes in TRPV3 expression and function was selected for the studies shown herein.

Statistical Analysis and Experimental Design: All experiments were designed to test a pre-planned hypothesis, with the exception of studies evaluating different types of wood/biomass smoke PM (Supp. Figs. 2 and 5) which were exploratory in nature. Data are represented as the mean ± SD. Significance was determined using ordinary one- or two-way ANOVA with Bonferroni correction at the 95% confidence level, unless otherwise stated.

Results:

Pine WSPM promotes cytotoxicity and activates TRPV3 and TRPA1 in lobar HBECs: Lobar HBECs were treated with increasing concentrations of pine WSPM for 24h. Pine WSPM caused dose-dependent cytotoxicity with an LD_{50} of ~18.8 μg/cm^2 (Figure 1A). Lobar cells were also treated with pine WSPM (78 μg/cm^2) to assess TRP channel activation using a short-term

Molecular Pharmacology Fast Forward. Published on September 16, 2020 as DOI: 10.1124/molpharm.120.000047
This article has not been copyedited and formatted. The final version may differ from this version.

(100 s) calcium flux assay (Figure 1B). Small (~10% ionomycin), but significant changes in cytosolic calcium were observed immediately following WSPM treatment. This response was partially inhibited (~50%) by co-treating cells with the TRPA1 antagonist A967079 (20 μM) and ~70% using the TRPV3 antagonist 2-(5-trifluoromethyl-pyridine-2-ylsulfanyl)-1-(8-methyl-3,4-dihydro-2H-quinolin-1-yl)-ethanone (10 μM), which we will refer to as the/a "TRPV3 antagonist" throughout the remainder of the manuscript. Figure 1B shows that both TRPA1 and TRPV3 are activated by pine WSPM in lobar HBECs, while supplemental Figure 1 (Supp. Fig. 1) shows that neither A967079 nor the TRPV3 antagonist alone elicited calcium flux in these cells.

TRPA1 primarily localizes to the cell surface, while TRPV3 is expressed on the ER of HBECs: The sub-cellular localization of TRPA1 and TRPV3 in HBECs was not known, and locations could be critical for understanding mechanisms of cytotoxicity in HBECs treated with WSPM and agonists of these ion channels. Despite numerous attempts, TRPA1 localization by immunocytochemical methods was unsuccessful due to poor quality antibodies. Thus, TRPA1 localization was further evaluated using calcium flux assays and inhibitors of calcium influx versus intracellular/ER release (Figure 2A). Calcium flux elicited by the selective TRPA1 agonist AITC was attenuated >95% by co-treating cells with the extracellular calcium chelator EGTA and the cell-impermeable, non-selective TRP channel blocker, ruthenium red (RR), as previously described (Thomas *et al.*, 2007; Deering-Rice *et al.*, 2015). Control data for EGTA/RR are also shown in Supplemental Figure 1 (Supp. Fig. 1). Thapsigargin pre-treatment (5 min), used to deplete ER Ca^{2+}, only partially (~50%) attenuated calcium flux. These results suggest that TRPA1 resides on both the cell surface and the ER of cells, but that there may be a functional link between cell surface TRPA1 activation and ER calcium release.

Molecular Pharmacology Fast Forward. Published on September 16, 2020 as DOI: 10.1124/molpharm.120.000047
This article has not been copyedited and formatted. The final version may differ from this version.

Unlike AITC, calcium flux elicited by pine WSPM and carvacrol, which activate both TRPA1 and TRPV3, were only partially attenuated by EGTA and ruthenium red co-treatment (~25-50%), and to a much greater extent by thapsigargin pre-treatment (~70-90%) (Figure 2A). These results suggest that TRPV3 may reside within cells and contribute to the release of ER calcium by pine WSPM and carvacrol.

Immunocytochemical analysis of TRPV3 in lobar HBECs revealed overlapping staining with the ER-specific biomarker calnexin (Figure 2B and Supp. Fig. 3A). In agreement with this pattern of staining, calcium flux elicited by the selective TRPV3 agonist drofenine (250 μM; Figure 2A) (Deering-Rice *et al.*, 2014), was attenuated ~85% with thapsigargin pre-treatment, but <2% by EGTA and ruthenium red. These data suggest that the majority of TRPV3 is expressed on the ER, and the cumulative results are consistent with both TRPA1 and TRPV3 regulating calcium flux elicited by pine WSPM (as in Figure 1B), whereby TRPA1 contributes mainly to the EGTA/ruthenium red-sensitive (i.e., cellular influx) component, and both TRPA1 and TRPV3 regulate ER calcium release.

Pine WSPM induces a robust ERS response in HBECs: Based on the finding that pine WSPM caused ER calcium release, HBECs were treated with pine WSPM (20 μg/cm^2) and total mRNA was isolated at various times after treatment, to assess the expression of prototypical ERS-associated biomarkers; readers are directed to Scheme 1 as a reference for how each biomarker is involved in the overall integrated ERS response. Treated cells demonstrated marked time-dependent upregulation of the PERK/eIF2αK3 pathway biomarkers ATF3 and DDIT3, marked and transient up-regulation of the chaperone HSPA1A, and a gradual and sustained increase in XBP1 mRNA splicing indicative of IRE1α/β activation (Figures 3A-E). As expected, XBP1 splicing was rapid, occurring within 2h, followed by HSPA1A induction at 4h, whereas PERK-

Molecular Pharmacology Fast Forward. Published on September 16, 2020 as DOI: 10.1124/molpharm.120.000047
This article has not been copyedited and formatted. The final version may differ from this version.

dependent induction of ATF3 and DDIT3 mRNA was delayed, occurring at times >4h. Induction of ERS, assessed using DDIT3 and ATF3 induction, by a variety of WSPM materials (Supp. Fig. 2), as well as DDIT3 induction in HBEC3-KTs (38 ± 4-fold) and SAECs (6.23 ± 0.06-fold) was also observed following pine WSPM treatment, indicating that ERS is a common consequence of exposure of HBECs to WSPM, with the most potent TRPA1/TRPV3 agonists generally producing the greatest effects.

TRPV3 and TRPA1 activity differentially modulate pine WSPM-induced ERS: To determine the contributions of TRPA1 and TRPV3 to pine WSPM-induced ERS, cells were treated with pine WSPM (20 μg/cm^2) in the absence or presence of TRPA1 or TRPV3 antagonists for 24h. Inhibition of TRPA1 with A967079 (20 μM) partially (~30-40%) attenuated ERS, measured using DDIT3, ATF3, and HSPA1A induction (Figures 4A-C). However, XBP1 splicing was slightly exacerbated (Figure 4D). Similar results were observed using carvacrol, a TRPA1/TRPV3 agonist that mimics the activity of pine WSPM (Figures 4A-D). Alternatively, inhibition of TRPV3 generally resulted in an exacerbation of ERS using the same indices (Figures 4A-D). As shown in Supplemental Figure 4 (Supp. Fig. 4), similar trends for TRPA1 and TRPV3 inhibition were observed using coniferaldehyde (a component of pine WSPM) as a TRPA1 agonist, whereas neither antagonist universally affected cellular responses to drofenine, a selective TRPV3 agonist. Collectively, these results show that TRPA1 initiates ERS in response to pine WSPM and "chemical mimics" (i.e., carvacrol and coniferaldehyde) treatments, while TRPV3 attenuates these effects; TRPV3 activation alone had only minimal effects on ERS biomarker induction. These data suggest disparate roles for TRPA1 and TRPV3 in regulating ERS.

Pine WSPM modulates TRPA1 and TRPV3 expression during ERS: Lobar HBECs were treated with pine WSPM (20 μg/cm^2) for various times up to 24h. Previous work has shown that

Molecular Pharmacology Fast Forward. Published on September 16, 2020 as DOI: 10.1124/molpharm.120.000047
This article has not been copyedited and formatted. The final version may differ from this version.

lobar HBECs basally express TRPA1 at ~10 copies per 100,000 copies of β2M and TRPV3 at ~110 copies per 100,000 copies of β2M (Deering-Rice *et al.*, 2018). Here, relative to the control cells in which a slight induction of TRPA1 was observed, TRPA1 transcripts remained low over time following pine WSPM treatment (Figure 5A). Alternatively, TRPV3 transcripts were rapidly and transiently upregulated after pine WSPM treatment (up to ~150-fold greater than control), and remained elevated (~20-fold control cells) for up to 24h (Figure 5B). We hypothesize these changes in TRPA1 and TRPV3 may reflect adaptive changes in cells, representing a purposeful effort to decrease the deleterious effects of TRPA1 activation, while promoting TRPV3 function to counteract the pro-cytotoxic effects associated with TRPA1 activation and pathological ERS. Similar to ERS biomarkers, TRPV3 transcripts were also upregulated by a variety of WSPM sub-types (Supp. Fig. 5), as well as 19 ± 2 fold in HBEC-3KT cells treated with pine WSPM, suggesting again that this effect is a common response of HBECs to WSPM of various origins.

Overexpression of TRPV3 confers resistance to ERS in HBECs: To further understand the significance of TRPV3 induction during ERS, TRPV3OE cells were studied. BEAS-2B and TRPV3OE cells were treated with increasing concentrations of pine WSPM (1, 5, and 20 μg/cm^2) and a variety of prototypical ERS-inducing agents for 4h. The cells were then assayed for changes in mRNA for ERS biomarkers using qPCR (Table 1). Specifically, in response to the majority of the ERS-inducing agents tested, TRPV3OE cells exhibited reduced levels of DDIT3 and ATF3 induction, as well as decreased XBP1 splicing (XBP1s/XBP1u). Interestingly, HSPA1A induction appeared to be specifically associated with pine WSPM treatment. Collectively, these data imply a unique and broadly relevant role of TRPV3 in fettering the pathological PERK-dependent ERS branch, and presumably the associated pathological endpoints.

Molecular Pharmacology Fast Forward. Published on September 16, 2020 as DOI: 10.1124/molpharm.120.000047
This article has not been copyedited and formatted. The final version may differ from this version.

TRPV3 overexpression alters ERS-induced cell cycle arrest: A hallmark of PERK-activation during ERS is cell cycle arrest, particularly in the G2 phase. BEAS-2B and TRPV3OE cells were treated with thapsigargin (1 μM) or pine WSPM (5 μg/cm^2; 0.011 mg/mL pine WSPM solution) for 4h and assayed for cell-cycle distribution by flow cytometry (Figure 6). Both thapsigargin and pine WSPM caused cell cycle arrest at G2 in BEAS-2B cells. However, TRPV3OE cells exhibited a shift to S-phase in response to both treatments. This shift away from arrest at G2 indicates a reduction in cell cycle arrest and a fundamental alteration in cellular programming associated with the PERK-driven pathological, pro-apoptotic branch of the ERS response.

TRPV3 knockdown sensitizes cells to ERS elicited by pine WSPM: To further explore the hypothesis that TRPV3 is protective in the context of pathological ERS and pneumotoxic WSPM expsoure, BEAS-2B cells stably over-expressing shRNA targeting TRPV3 or a "scrambled" control shRNA were treated with either vehicle or pine WSPM at 20 μg/cm^2 for 4h, or 10 μg/cm^2 for 20h; doses were adjusted slightly to account for differences in sensitivity of BEAS-2B cells vs. lobar HBECs to the pine WSPM. The scrambled shRNA control BEAS-2B cells basally expressed 4.1 ± 0.7 copies of TRPV3 per 100,000 copies of β2M. As expected, TRPV3 mRNA was reduced ~50-60% in the TRPV3 shRNA knockdown cells, to levels essentially at the limit of detection of the qPCR assay (Figure 7A and C). Further, in control cells, pine WSPM induced TRPV3 mRNA expression, which was not observed in the TRPV3 shRNA-knockdown cells at 4h, and was attenuated ~50% at 20h. Finally, similar to the pharmacological inhibition data, shRNA-mediated knockdown of TRPV3 exacerbated ERS, measured using DDIT3 induction as an indicator of pathological ERS at 4 and 20h post pine WSPM treatment (Figure 7B and D).

Molecular Pharmacology Fast Forward. Published on September 16, 2020 as DOI: 10.1124/molpharm.120.000047
This article has not been copyedited and formatted. The final version may differ from this version.

Effects of TRPA1 and TRPV3 inhibition on WSPM cytotoxicity: An ultimate goal of this study was to determine how and to what extent TRPA1 and TRPV3 regulated the cytotoxic effects of pneumotoxic WSPM in primary HBECs. As such, the effects of TRPA1 and TRPV3 inhibition were evaluated as inhibitors of cytotoxicity. Lobar HBECs were treated with pine WSPM at 20 $\mu g/cm^2$ for 24h with either the TRPA1 antagonist A967079 (20 μM) or the TRPV3 antagonist (10 μM); higher concentrations of the antagonists were tested, but as per prior publications by our group, the antagonists themselves became cytotoxic (Deering-Rice *et al.*, 2014, 2018; Memon *et al.*, 2020). Consistent with the cumulative findings on the modulation of pathological ERS by TRPA1 and TRPV3 activity, the cytotoxicity of pine WSPM was blocked by co-treating cells with the TRPA1 antagonist A967079 (20 μM), but was exacerbated (~2-fold) by TRPV3 inhibition (Figure 8). These findings demonstrate that TRPA1 and TRPV3 differentially regulate pathological ERS in HBECs, ultimately influencing the ability of cells to either adapt to and survive stress, or succumb to stress and die.

Effects of TRPA1 and TRPV3 inhibitors on calcium flux: Finally, to clarify the differential effects of TRPA1 and TRPV3 on ERS and cytotoxicity, the effects of the TRPA1 and TRPV3 antagonists on TRPA1- and TRPV3-driven calcium flux in both lobar HBECs and TRPA1 and TRPV3-overexpressing HEK-293 cells was tested following treatment with selective agonists of each channel. In lobar HBECs, TRPA1 inhibition by A967079 (20 μM) attenuated both TRPA1-driven calcium flux (~25-40%) by AITC (150 μM; Figure 9A) as well as TRPV3-driven calcium flux (~85-90%) by drofenine (250 μM; Figure 9B). However, TRPV3 inhibition by the TRPV3 antagonist (10 μM) attenuated only TRPV3-driven calcium flux (~50-60%) by drofenine (250 μM; Figure 9B) while enhancing (~3-fold) TRPA1-driven calcium flux by AITC (150 μM; Figures 9A and B). The effects of these antagonists were unique to HBEC cells, based the finding that neither

Molecular Pharmacology Fast Forward. Published on September 16, 2020 as DOI: 10.1124/molpharm.120.000047
This article has not been copyedited and formatted. The final version may differ from this version.

antagonist affected the other channel in TRPA1 or TRPV3-overexpressing HEK-293 cells (Figures 9C and D). Additionally, TRPA1 activation by a nonelectrophilic agonist, 2,4 *ditert*-butylphenol, was blocked by A967079 (20 μM) in TRPA1-overexpressing cells, indicating that the effects of A967079 on TRPA1 activity are independent of the agonist reactivity or mechanism of binding (Supp. Fig. 6). These results imply a functional coupling between TRPA1 and TRPV3 activities in HBECs, wherein TRPA1 stimulates TRPV3 and TRPV3 attenuates TRPA1, seemingly explaining the differential effects that TRPA1 and TRPV3 have on ERS and cytotoxicity.

Discussion:

The goals of this study were to further define mechanisms by which pneumotoxic WSPM affect HBEC viability using a primary lung cell model, and to elucidate roles for TRPA1 and TRPV3 in regulating ERS and cell death caused by WSPM, using pine WSPM as a model. This study identified differences in the subcellular localization and functional significance of TRPA1 and TRPV3, both in the context of initiation of pathological ERS and the manifestation of cytotoxicity; revealing atypical and contrasting roles. Specifically, TRPA1 activation was found to initiate pathological, PERK-driven ERS, indicated by increases in the expression of established biomarkers of this pathway (i.e., pro-apoptotic DDIT3 and ATF3), cell cycle arrest at G2, and cell death. In contrast, a novel and unexpected role for TRPV3 as a negative regulator of PERK-dependent pathological ERS following pine WSPM, TRPA1 agonist, and prototypical ERS-inducing agent treatments, was revealed. Finally, changes in TRPA1 and TRPV3 mRNA expression were observed in HBECs following treatment with pine PM and multiple other forms of WSPM, highlighting a potential common mechanism by which pneumotoxic substances that either directly activate TRPA1 or TRPV3, and/or produce ERS, might affect HBECs. Consistent

Molecular Pharmacology Fast Forward. Published on September 16, 2020 as DOI: 10.1124/molpharm.120.000047
This article has not been copyedited and formatted. The final version may differ from this version.

with this idea, we have previously hypothesized that differences in the relative abundance of TRPA1 and TRPV3 agonists in certain samples of DEP emissions (i.e., 2,4 *ditert*-butylphenol) may influence the relative pro-inflammatory potential of these materials in HBECs and animal models (Deering-Rice *et al.*, 2019).

The specific contributions of TRPA1 and TRPV3 in regulating ERS and cytotoxicity were initilally puzzling. It was found that TRPA1 localized to both the cell surface and ER, while the majority of TRPV3 was associated with the ER. Yet, only TRPA1 was ultimately found to initiate pathological ERS and cytotoxicity caused by pine WSPM and other TRPA1 agonists, while TRPV3 seemed to conteract this effect, despite being activated by pine WSPM, and the selective TRPV3 agonist drofenine, which generally did not induce a robust ERS response despite triggering ER calcium release. Influx of calcium into cells from extracellular sources is not typically associated with ERS. Thus, it is likely that the ER sub-population of TRPA1 selectively drives the ERS responses observed following treatment with WSPM and other TRPA1 agonists. It is also possible that cell surface TRPA1 activation may promote ER calcium release through other ER calcium release channels such as ryanodine receptors and/or IP3 receptors, as suggested by others (Pan *et al.*, 2016; Xu *et al.*, 2017), to promote ERS. The finding that AITC-driven calcium flux in HBEC cells was only partially inhibited by thapsigargin pre-treatment, but extensively inhibited by EGTA and ruthenium red supports such a possibility.

Another hypothesis directly supported by the experimental data is that TRPA1 activation in HBECs stimulates TRPV3 activity to enhance ER calcium release, which in combination would explain the robust ERS responses observed with the WSPM and carvacrol, relative to more selective TRPA1 (i.e., AITC and coniferaldehyde) or TRPV3 (drofenine) agonists. Sensitization of TRPV3 by cytosolic calcium has been described, resulting from a reduction in calmodulin

Molecular Pharmacology Fast Forward. Published on September 16, 2020 as DOI: 10.1124/molpharm.120.000047
This article has not been copyedited and formatted. The final version may differ from this version.

binding, which normally inhibits the channel (Nilius *et al.*, 2014). Accordingly, pine WSPM-induced increases in cytosolic calcium via TRPA1 may sensitize TRPV3, which in turn would enhance ER calcium depletion and trigger a robust ERS response, as observed for carvacrol and pine WSPM, but not drofenine or coniferaldehyde. High intracellular calcium would also promote TRPA1 desensitization to temper TRPA1 activity (Ruparel *et al.*, 2011; Memon *et al.*, 2020), TRPV3 activity, and ultimately ERS, seemingly explaining how TRPV3 can reduce ERS caused by TRPA1 and TRPA1/TRPV3 agonists (Scheme 2).

Another intriguing finding was that the inhibitory effect of TRPV3 overexpression on ERS was not only limited to pine WSPM or TRP channel agonist treatment, suggesting that TRPV3 may play previously unrecognized roles in regulating the toxicity of a variety of agents. Specifically, TRPV3OE cells exhibited diminished pathological ERS in comparison to BEAS-2B cells, following treatment with multiple distinct ERS-inducing agents including an ER calcium depleting agent (thapsigargin), an inhibitor of glucose metabolism (2-deoxy-D-glucose), oxidative and reductive stress-inducing agents (H_2O_2 and DTT), a glycosylation inhibitor (tunicamycin), and the UPR/proteasomal inhibitor (Eeyarestatin-I). In general, TRPV3 over-expression conferred protection against ERS induced by most of these agents, based on decreases in the level of DDIT3 induction (i.e., the pro-apoptotic branch of the ERS response). These data imply a possible selective effect of TRPV3 on PERK-dependent signaling, which may result from TRPV3 promoting calcium homeostasis, as has been suggested for TRPC1 in salivary gland cells (Sukumaran *et al.*, 2019). Accordingly, the induction of TRPV3 in conjunction with suppressed TRPA1 expression may indicate a deliberate process by which cells attempt to restore the balance of ER and cytosolic calcium concentrations to limit ERS and other pathological processes, wherein TRPA1 and TRPV3 play central roles. Regardless of the precise mechanism by which TRPV3

protects cells against ERS, it is clear that TRPV3 does protect cells against the deleterious effects of initiating a robust and prolonged ERS response that leads to cell cycle arrest and cytotoxicity.

Finally, regarding the primary conclusions of this study, our group previously reported that TRPV3 overexpression sensitized BEAS-2B cells to WSPM-induced cytotoxicity, and that cells could be protected using a TRPV3 antagonist (Deering-Rice *et al.*, 2018). As such, the inhibitory roles of TRPV3 in pathological ERS and exacerbation of cell death observed here, contradict our initial hypothesis that TRPV3 would promote WSPM toxicity through an ERS-dependent mechanism. Primary HBECs are a more relevant model of the human airway epithelium and the collective data reported here suggest that our initial hypothesis about TRPV3, based on TRPV3-OE cells, was simply incorrect, and several key differences between TRPV3OE and normal cells may explain this discrepency. TRPV3-overexpressing cells lack the ability to control TRPV3 expression during stress. As such, the levels of TRPV3 in the TRPV3OE cells are supraphysiological, and static. This is not without consequence, and we have observed a down-regulation in the basal levels of key ERS response genes in the TRPV3OE cells in transcriptome analyses, suggesting that downregulating ERS machinery may limit the ability of cells to engage early cellular defenses against stress and to adapt to and compensate for and overcome the stress. Additionally, TRPA1 activation by AITC was not observed with TRPV3OE cells despite expressing higher levels of mRNA than normal BEAS-2B and primary HBECs. As per scheme 2, this may be due to calcium-dependent inhibition of TRPA1 by basal TRPV3 activity, rendering TRPA1 essentially incapable of initiating ERS. Finally, a portion of TRPV3 is expressed on the cell surface of TRPV3-OE cells. Consequently, TRPV3OE cells likely die via a mechanism independent of ERS when treated with WSPM, which is not replicated in primary HBECs.

Molecular Pharmacology Fast Forward. Published on September 16, 2020 as DOI: 10.1124/molpharm.120.000047
This article has not been copyedited and formatted. The final version may differ from this version.

To summarize, this study provides new mechanistic insights into how pneumotoxic WSPM, agonists of TRPA1, and possibly other toxic agents can adversely affect HBECs. These formative findings are among the first to describe such roles for TRPA1 and TRPV3 in HBECs and provide new insights into both normal physiological and pathophysiological functions associated with these receptors in the lung epithelium, particularly in the context of WSPM-induced lung cell injury. Significant results include the identification of seemingly opposing roles for TRPA1 and TRPV3 in regulating ERS and cell death in response to pine WSPM, and that TRPV3 may be critical in limiting ERS independent of the stimulus via coordinated induction during ERS. Finally the protective effect of TRPV3 appears to be through activity-dependent inhibition of TRPA1 and specific modulation of the PERK-dependent pro-apoptotic branch of the ERS signaling network involving DDIT3. While additional work is needed to determine the broader significance of this signaling nexus in lung injury, these findings advance our general understanding of how these TRP channels regulate lung cell responses to toxicants such as WSPM.

Declaration of Conflicts of Interest

The authors declare no potential conflicts of interest with respect to the research, authorship, and/or publication of this article.

Acknowledgements:

The authors acknowledge the DNA/Peptide Core of the University of Utah Health Sciences Cores for synthesizing and HPLC-purifying primers and probes, as well as the Synthetic and

Medicinal Chemistry Core for synthesizing the TRPV3 antagonist. The authors would also like to thank Ms. Katherine Rose for technical assistance with this work and Dr. Kevin D. Welch, PhD of the USDA Agricultural Research Services in Logan, UT for assistance in obtaining the animal feces samples.

Author Contributions:
Participated in research design: Nguyen, Memon, Burrell, Deering-Rice, Reilly
Conducted experiments: Nguyen, Memon, Burrell, Almestica-Roberts, Rapp, Sun, Scott, Deering-Rice, Reilly
Performed data analysis: Nguyen, Memon, Almestica-Roberts, Rapp, Sun, Deering-Rice, Rower, Reilly
Wrote or contributed to writing of the manuscript: Nguyen, Memon, Burrell, Almestica-Roberts, Rapp, Scott, Deering-Rice, Rower, Reilly
Obtained funding for the research: Deering-Rice, Reilly

References:

Andrè E, Campi B, Materazzi S, Trevisani M, Amadesi S, Massi D, Creminon C, Vaksman N, Nassini R, Civelli M, Baraldi PG, Poole DP, Bunnett NW, Geppetti P, and Patacchini R (2008) Cigarette smoke–induced neurogenic inflammation is mediated by α,β-unsaturated aldehydes and the TRPA1 receptor in rodents. *J Clin Invest* **118**:2574–2582, American Society for Clinical Investigation.

Bessac BF, Sivula M, Von Hehn CA, Escalera J, Cohn L, and Jordt SE (2008) TRPA1 is a major oxidant sensor in murine airway sensory neurons. *J Clin Invest* **118**:1899–1910.

Deering-Rice CE, Johansen ME, Roberts JK, Thomas KC, Romero EG, Lee J, Yost GS, Veranth JM, and Reilly CA (2012) Transient receptor potential vanilloid-1 (TRPV1) is a mediator of lung toxicity for coal fly ash particulate material. *Mol Pharmacol* **81**:411–419.

Deering-Rice CE, Memon T, Lu Z, Romero EG, Cox J, Taylor-Clark T, Veranth JM, and Reilly CA (2019) Differential Activation of TRPA1 by Diesel Exhaust Particles: Relationships between Chemical Composition, Potency, and Lung Toxicity. *Chem Res Toxicol* **32**:1040–1050, American Chemical Society.

Deering-Rice CE, Mitchell VK, Romero EG, Abdel Aziz MH, Ryskamp DA, Križaj D, Venkat RG, and Reilly CA (2014) Drofenine: a 2-APB analog with improved selectivity for human TRPV3. *Pharmacol Res Perspect* **2**:e00062.

Deering-Rice Cassandra E, Nguyen N, Lu Z, Cox JE, Shapiro D, Romero EG, Mitchell VK, Burrell KL, Veranth JM, and Reilly CA (2018) Activation of TRPV3 by Wood Smoke Particles and Roles in Pneumotoxicity. *Chem Res Toxicol* **31**:301.

Deering-Rice Cassandra E., Nguyen N, Lu Z, Cox JE, Shapiro D, Romero EG, Mitchell VK, Burrell KL, Veranth JM, and Reilly CA (2018) Activation of TRPV3 by Wood Smoke

Particles and Roles in Pneumotoxicity. *Chem Res Toxicol* **31**:291–301, American Chemical Society.

Deering-Rice CE, Romero EG, Shapiro D, Hughen RW, Light AR, Yost GS, Veranth JM, and Reilly CA (2011) Electrophilic components of diesel exhaust particles (DEP) activate transient receptor potential ankyrin-1 (TRPA1): a probable mechanism of acute pulmonary toxicity for DEP. *Chem Res Toxicol* **24**:950–9, NIH Public Access.

Deering-Rice CE, Shapiro D, Romero EG, Stockmann C, Bevans TS, Phan QM, Stone BL, Fassl B, Nkoy F, Uchida DA, Ward RM, Veranth JM, and Reilly CA (2015) Activation of Transient Receptor Potential Ankyrin-1 by Insoluble Particulate Material and Association with Asthma. *Am J Respir Cell Mol Biol* **53**:893–901.

Deering-Rice CE, Stockmann C, Romero EG, Lu Z, Shapiro D, Stone BL, Fassl B, Nkoy F, Uchida DA, Ward RM, Veranth JM, and Reilly CA (2016) Characterization of Transient Receptor Potential Vanilloid-1 (TRPV1) variant activation by coal fly ash particles and associations with altered Transient Receptor Potential Ankyrin-1 (TRPA1) expression and asthma. *J Biol Chem* **291**:24866–24879, American Society for Biochemistry and Molecular Biology Inc.

Ghio AJ, Soukup JM, Case M, Dailey LA, Richards J, Berntsen J, Devlin RB, Stone S, and Rappold A (2012) Exposure to wood smoke particles produces inflammation in healthy volunteers. *Occup Environ Med* **69**:170–175.

Kim YH, Warren SH, Krantz QT, King C, Jaskot R, Preston WT, George BJ, Hays MD, Landis MS, Higuchi M, Demarini DM, and Gilmour MI (2018) Mutagenicity and lung toxicity of smoldering vs. Flaming emissions from various biomass fuels: Implications for health effects from wildland fires. *Environ Health Perspect* **126**, Public Health Services, US Dept

of Health and Human Services.

Korfei M, Ruppert C, Loeh B, Mahavadi P, and Guenther A (2016) The role of Endoplasmic Reticulum (ER) stress in pulmonary fibrosis. *Endoplam Reticul Stress Dis* **3**:16–49.

Laumbach RJ, and Kipen HM (2012) Respiratory health effects of air pollution: Update on biomass smoke and traffic pollution. *J Allergy Clin Immunol* **129**:3–11, Mosby.

Liu JC, Wilson A, Mickley LJ, Dominici F, Ebisu K, Wang Y, Sulprizio MP, Peng RD, Yue X, Son JY, Anderson GB, and Bell ML (2017) Wildfire-specific fine particulate matter and risk of hospital admissions in urban and rural counties. *Epidemiology* **28**:77–85, Lippincott Williams and Wilkins.

Maiuolo J, Bulotta S, Verderio C, Benfante R, and Borgese N (2011) Selective activation of the transcription factor ATF6 mediates endoplasmic reticulum proliferation triggered by a membrane protein. *Proc Natl Acad Sci U S A* **108**:7832–7837.

Martino MB, Jones L, Brighton B, Ehre C, Abdulah L, Davis CW, Ron D, O'Neal WK, and Ribeiro CMP (2013) The ER stress transducer IRE1β is required for airway epithelial mucin production. *Mucosal Immunol* **6**:639–654.

Memon TA, Nguyen ND, Burrell KL, Scott AF, Almestica-Roberts M, Rapp E, Deering-Rice CE, and Reilly CA (2020) Wood Smoke Particles Stimulate MUC5AC Overproduction by Human Bronchial Epithelial Cells through TRPA1 and EGFR Signaling. *Toxicol Sci*, doi: 10.1093/toxsci/kfaa006.

Nilius B, Bíró T, and Owsianik G (2014) TRPV3: time to decipher a poorly understood family member! *J Physiol* **592**:295–304, Wiley/Blackwell (10.1111).

Olloquequi J, and Silva R (2016) Biomass smoke as a risk factor for chronic obstructive pulmonary disease: effects on innate immunity. *Innate Immun* **22**:373–381, SAGE

PublicationsSage UK: London, England.

Pan Y, Zhao G, Cai Z, Chen F, Xu D, Huang S, Lan H, and Tong Y (2016) Synergistic effect of ferulic acid and Z-ligustilide, major components of A. sinensis, on regulating cold-sensing protein TRPM8 and TPRA1 in vitro. *Evidence-based Complement Altern Med* **2016**, Hindawi Publishing Corporation.

Reid CE, Jerrett M, Tager IB, Petersen ML, Mann JK, and Balmes JR (2016) Differential respiratory health effects from the 2008 northern California wildfires: A spatiotemporal approach. *Environ Res* **150**:227–235, Academic Press Inc.

Ruparel NB, Patwardhan AM, Akopian AN, and Hargreaves KM (2011) Desensitization of transient receptor potential ankyrin 1 (TRPA1) by the TRP vanilloid 1-selective cannabinoid arachidonoyl-2 chloroethanolamine. *Mol Pharmacol* **80**:117–123, American Society for Pharmacology and Experimental Therapeutics.

Shapiro D, Deering-Rice CE, Romero EG, Hughen RW, Light AR, Veranth JM, and Reilly CA (2013) Activation of transient receptor potential ankyrin-1 (TRPA1) in lung cells by wood smoke particulate material. *Chem Res Toxicol*, doi: 10.1021/tx400024h.

Sukumaran P, Sun Y, Zangbede FQ, Nascimento da Conceicao V, Mishra B, and Singh BB (2019) TRPC1 expression and function inhibit ER stress and cell death in salivary gland cells. *FASEB BioAdvances* **1**:40–50.

Swiston JR, Davidson W, Attridge S, Li GT, Brauer M, and Van Eeden SF (2008) Wood smoke exposure induces a pulmonary and systemic inflammatory response in firefighters. *Eur Respir J* **32**:129–138.

Thomas KC, Ethirajan M, Shahrokh K, Sun H, Lee J, Cheatham TE, Yost GS, Reilly CA, and Reilly CA (2011) Structure-activity relationship of capsaicin analogs and transient receptor

potential vanilloid 1-mediated human lung epithelial cell toxicity. *J Pharmacol Exp Ther* **337**:400–10, American Society for Pharmacology and Experimental Therapeutics.

Thomas KC, Roberts JK, Deering-Rice CE, Romero EG, Dull RO, Lee J, Yost GS, and Reilly CA (2012) Contributions of TRPV1, endovanilloids, and endoplasmic reticulum stress in lung cell death in vitro and lung injury. *Am J Physiol Lung Cell Mol Physiol* **302**:L111-9, American Physiological Society.

Thomas KC, Sabnis AS, Johansen ME, Lanza DL, Moos PJ, Yost GS, and Reilly CA (2007) Transient receptor potential vanilloid 1 agonists cause endoplasmic reticulum stress and cell death in human lung cells. *J Pharmacol Exp Ther* **321**:830–838, J Pharmacol Exp Ther.

Wang Y, Wu Z-Z, and Wang W (2017) Inhibition of endoplasmic reticulum stress alleviates cigarette smoke-induced airway inflammation and emphysema. *Oncotarget* **8**:77685–77695, Impact Journals, LLC.

Watterson TL, Hamilton B, Martin R, and Coulombe RA (2009) Urban Particulate Matter Causes ER Stress and the Unfolded Protein Response in Human Lung Cells. *Toxicol Sci* **112**:111–122.

Xu C, Bailly-Maitre B, and Reed JC (2005) Endoplasmic reticulum stress: Cell life and death decisions.

Xu C, Luo J, He L, Montell C, and Perrimon N (2017) Oxidative stress induces stem cell proliferation via TRPA1/RyR-mediated Ca2+signaling in the Drosophila midgut. *Elife* **6**, eLife Sciences Publications Ltd.

Xu M, Zhang Yanbei, Wang M, Zhang H, Chen Y, Adcock IM, Chung KF, Mo J, Zhang Yinping, and Li F (2019) TRPV1 and TRPA1 in Lung Inflammation and Airway Hyperresponsiveness Induced by Fine Particulate Matter ($PM_{2.5}$). *Oxid Med Cell Longev*

2019:1–15, Hindawi.

Yao Y, Wang Y, Zhang Z, He L, Zhu J, Zhang M, He X, Cheng Z, Ao Q, Cao Y, Yang P, Su Y, Zhao J, Zhang S, Yu Q, Ning Q, Xiang X, Xiong W, Wang CY, and Xu Y (2016) Chop deficiency protects mice against bleomycin-induced pulmonary fibrosis by attenuating M2 macrophage production. *Mol Ther* **24**:915–925, Nature Publishing Group.

Footnotes:

This work was supported by National Institute of Environmental Health Sciences grants [ES017431] and [ES027015]. Nam Nguyen was supported in part by a University of Utah Undergraduate Research Opportunities award, and Marysol Almestica-Roberts was supported by a National Institute of General Medical Sciences Diversity Supplement award associated with grant [GM121648]. Katherine Burrell received partial support from a University of Utah ARUP fellowship. Imaging was performed at the Florescence Microscopy Core Facility, a part of the Health Sciences Cores at the University of Utah. Microscopy equipment was obtained using a National Center for Research Resources Shared Equipment Grant [RR024761]. The University of Utah Flow Cytometry Facility is supported by the National Cancer Institute Award Number [CA042014].

Molecular Pharmacology Fast Forward. Published on September 16, 2020 as DOI: 10.1124/molpharm.120.000047
This article has not been copyedited and formatted. The final version may differ from this version.

Figure Legends:

Figure 1: WSPM cytotoxicity and the contributions of TRPV3 and TRPA1 in regulating pine WSPM-induced calcium flux. **(A)** Changes in lobar HBEC viability following 24h treatment with increasing concentrations of pine WSPM. Data are represented as the mean percentage (± SD) of residual viability compared to untreated control for n=3 replicates. **(B)** Inhibition of pine WSPM-induced calcium flux in lobar HBECs treated with pine WSPM (78 μg/cm^2) with or without the TRPA1 antagonist A967079 (20 μM) or the "TRPV3 antagonist" 2-(5-trifluoromethyl-pyridine-2-ylsulfanyl)-1-(8-methyl-3,4-dihydro-2H-quinolin-1-yl)-ethanone (10 μM). Calcium flux data were recorded over a 100-second period and values for vehicle treatment were subtracted and then normalized to the maximum fluorescence change elicited by ionomycin (10 μM). Data represent the mean ± SD for n≥3 replicates. ***, p<0.001, ****. P<0.0001 using an ordinary ANOVA with a Dunnett multiple comparisons test versus pine WSPM only treatment.

Figure 2: Localization of TRPA1 and TRPV3 in HBECs. **(A)** Functional expression of TRPA1 and TRPV3 in lobar HBECs using a calcium flux assay. Agonists of TRPA1 (allyl isothiocyanate, AITC, 300 μM), TRPA1/TRPV3 (pine WSPM, 78 μg/cm^2, and carvacrol, 250 μM), and TRPV3 (drofenine, 250 μM), were used in combination with either the EGTA (50 μM) and ruthenium red (250 μM) to block the influx of extracellular calcium into cells, or thapsigargin (2.5 μM) to deplete intracellular/ER calcium stores. Calcium flux data (over a 100-second period) are represented as a percentage of the maximum fluorescence in the cells, elicited by the calcium ionophore ionomycin (10 μM). Data are represented as mean ± SD from n=3 replicates. *, p<0.05, **, p<0.01, and ****, p<0.0001 using ordinary two-way ANOVA and the Tukey post-test comparing each treatment to the respective agonist only control. **(B)** Representative immunostaining of TRPV3 (green), the ER

biomarker calnexin (red), and nuclei (blue) in lobar HBECs. The complete fluorescence micrographs may be found in Supplemental Figure 3.

Figure 3: Temporal profiling of ERS biomarkers in lobar HBECs in response to pine WSPM treatment. Expression of mRNA for the ERS biomarkers **(A)** ATF3, **(B)** DDIT3, **(C)** HSPA1A, and **(D)** spliced XBP1 by lobar HBECs during treatment with pine WSPM (20 μg/cm^2, filled circles) or vehicle (open circles) over time. Differences in the magnitude of induction should be noted. Each time point was normalized against the 0h vehicle-treated control and are presented as mean ± SD from n=3 replicates. (E) Western blots confirming the upregulation of DDIT3 and HSP70 proteins in pine WSPM-treated HBECs. ATF3 and TRPV3 were not detected by western blot; recently purchased TRPV3 antibody aliquots retain selectivity, but show marked decreases in sensitivity for detecting TRPV3 in lung cells. **, p<0.01; ***, p<0.001; ****, p<0.000 Statistical significance was determined using an ordinary two-way ANOVA using the Sidak multiple comparisons test.

Figure 4: Effects of TRPA1 or TRPV3 inhibition on pine WSPM-induced ERS biomarker induction. Expression of **(A)** ATF3, **(B)** DDIT3, **(C)** HSPA1A, and **(D)** spliced XBP1 mRNA 24h after treatment of lobar HBECs with pine WSPM (20 μg/cm^2) or carvacrol (250 μM), in the presence of either the TRPA1 antagonist A967079 (20 μM) or the TRPV3 antagonist (10 μM). Data were normalized to the vehicle-treated group and are represented as mean ± SD from n=3 replicates. Statistical significance was determined using an ordinary two-way ANOVA using the Tukey post-test comparing all treatments for each group. **, p<0.01; ***, p<0.001; ****, p<0.0001 relative to the respective no antagonist control. ###, p<0.001; ####, p<0.0001 indicates differences between the TRPA1 and TRPV3 antagonist groups.

Figure 5: Temporal changes in TRPA1 and TRPV3 mRNA expression following pine WSPM treatment. **(A)** TRPA1 and **(B)** TRPV3 mRNA expression over time in lobar HBECs during treatment with pine WSPM (20 μg/cm^2; filled circles) or vehicle (open circles). Each time point was normalized against the 0h vehicle-treated control and are represented as mean ± SD from n=3 replicates. Statistical significance was determined using an ordinary two-way ANOVA using the Sidak multiple comparisons test.

Figure 6: Effect of TRPV3 over-expression on ERS-associated cell cycle arrest. **(A)** Cell cycle analysis by flow cytometry on BEAS-2B cells or **(B)** TRPV3OE cells, following 4h treatment with either vehicle (white bars), thapsigargin (1 μM; black bars), or pine WSPM (5 μg/cm^2; grey bars). The data represent cells in a specific phase of the cell cycle as a percentage of total viable cells. Data are presented as the mean ± SD from n=3 replicates. **, p<0.01; ***, p<0.001; ****, p<0.0001. Statistical significance was determined using an ordinary two-way ANOVA with the Bonferonni correction.

Figure 7: Effects of shRNA-driven TRPV3 knockdown on the sensitivity of BEAS-2B cells to pine WSPM-induced ERS. mRNA expression of **(A**, **C)** TRPV3 and **(B, D)** DDIT3 in BEAS-2B cells stably overexpressing control/scrambled shRNA (white bars) or shRNA targeting TRPV3 (black bars) after 4h treatment with vehicle and pine WSPM (20 μg/cm^2) **(A, B)** or 20h treatment with vehicle and pine WSPM (10 μg/cm^2) **(C, D)**. Data were normalized to the vehicle-treated shTRPV3 cells and are presented as the mean ± SD from n=3 replicates. **, p<0.01, ***, p<0.001, ****, p<0.0001 compared to vehicle treated control cells, $^{\#}$, p<0.05, $^{\#\#}$, p<0.01,$^{\#\#\#}$, p<0.001, $^{\#\#\#\#}$, p<0.0001 compared to pine WSPM treated control cells, and ^, p<0.05, ^^^^, p<0.0001 compared

Molecular Pharmacology Fast Forward. Published on September 16, 2020 as DOI: 10.1124/molpharm.120.000047
This article has not been copyedited and formatted. The final version may differ from this version.

to vehicle-treated scramble control cells using an ordinary two-way ANOVA and the Tukey post-test comparing all data sets.

Figure 8: Effects of TRPA1 and TRPV3 inhibition on pine WSPM-induced cytotoxicity. Lobar HBEC viability was assayed after 24h of treatment with pine WSPM (20 μg/cm^2), in the presence of A967079 (20 μM, grey bars) or the TRPV3 antagonist (10 μM, black bars). Data were normalized against the vehicle control and are presented as the mean ± SD for n=3 replicates. *, $p<0.05$, ****, $p<0.0001$ compared to vehicle treated cells without an antagonist, $^{####}$, $p<0.0001$ compared to pine WSPM treatment without antagonists using an ordinary two-way ANOVA and the Dunnett post-test.

Figure 9: Functional interactions between TRPA1 and TRPV3 activities. **(A)** Alterations in TRPA1-mediated calcium flux in lobar HBECs treated with allyl isothiocyanate (AITC; 150 μM) with or without the TRPA1 antagonist A967079 (20 μM) or the TRPV3 antagonist (10 μM). **(B)** Inhibition of TRPV3-mediated calcium flux in lobar HBECs treated with drofenine (250 μM) with or without the TRPA1 antagonist A967079 (20 μM) or a TRPV3 antagonist (10 μM). Data are presented as the mean ± SEM from n≥5 replicates. **(C)** Effects of the TRPA1 and TRPV3 antagonists on TRPA1-mediated calcium flux elicited by allyl isothiocyante (AITC; 150 μM) in TRPA1-overexpressing HEK-293 cells. **(D)** Effects of the TRPA1 and TRPV3 antagonists on TRPV3-mediated calcium flux by drofenine (250 μM) in TRPV3-overexpressing HEK-293 cells. Data are presented as the mean ± SD from n≥3 replicates. *, $p<0.05$, **, $p<0.01$, ***, $p<0.001$, ****, $p<0.0001$ using an ordinary one-way ANOVA with the Bonferroni correction.

Table 1: Effects of TRPV3 overexpression on BEAS-2B cell responses to pine WSPM and prototypical ERS-inducing agents.

Treatment	ATF3		DDIT3		HSPA1A		XBP1s/XBP1u	
	BEAS-2B	TRPV3OE	BEAS-2B	TRPV3OE	BEAS-2B	TRPV3OE	BEAS-2B	TRPV3OE
Vehicle	1.0 ± 0.3	1.2 ± 0.4	1.0 ± 0.2	1.2 ± 0.2	1.0 ± 0.0	0.4 ± 0.0	1.0 ± 0.2	0.8 ± 0.2
Pine WSPM (1 μg/cm^2)	2.2 ± 0.7	3.4 ± 0.4	**4.3 ± 0.7**	**2.0 ± 0.3***	**4.4 ± 0.3**	**0.9 ± 0.3***	2.8 ± 0.5	1.3 ± 0.1
Pine WSPM (5 μg/cm^2)	*6.1 ± 0.9*	*12 ± 1**	**12 ± 2**	**3.9 ± 0.5***	**24 ± 2**	**7 ± 2***	2.4 ± 0.6	0.9 ± 0.1
Pine WSPM (20 μg/cm^2)	**40 ± 4**	**7 ± 1***	**17 ± 2**	**4 ± 1***	**16.0 ± 0.2**	**1.7 ± 0.2***	9 ± 2	1.0 ± 0.1
Thapsigargin (10 μM)	**95 ± 7**	**33 ± 13***	**46 ± 2**	**33 ± 7**	0.1 ± 0.0	0.1 ± 0.0	**18.2 ± 0.9**	**8 ± 2***
DTT (250 μM)	*2.4 ± 0.2*	*12 ± 1**	**15.0 ± 0.2**	**10.2 ± 0.8***	0.2 ± 0.3	0.4 ± 0.3	**4.9 ± 0.1**	**2.9 ± 0.2***
Eeyarestatin I (4 μM)	15 ± 2	18 ± 3	**21 ± 2**	**15 ± 1***	0.9 ± 0.6	2.7 ± 0.6	3.1 ± 0.5	1.9 ± 0.1
Tunicamycin (2.5 μg/mL)	12 ± 2	17 ± 2	**59 ± 8**	**41 ± 3**	0.1 ± 0.0	0.1 ± 0.0	22 ± 2	12 ± 3
H_2O_2 (1 mM)	**4.7 ± 0.4**	**1.1 ± 0.2***	**10.5 ± 0.9**	**4.0 ± 0.6***	0.1 ± 0.0	0.4 ± 0.0	1.3 ± 0.3	1.0 ± 0.2
2-Deoxy-D-Glucose (10 mM)	**25 ± 4**	**11.7 ± 0.5***	**49 ± 6**	**22 ± 2***	0.3 ± 0.0	0.1 ± 0.0	9 ± 3	3.6 ± 0.3

Relative expression of mRNA for ERS biomarkers in BEAS-2B (B2B) and TRPV3OE cells, following 4h treatment with various ERS-Inducing agents. Data are presented as relative mRNA expression, normalized to vehicle-treated BEAS-2B cells and are represented as the mean ± SD from n=3 replicates. *Indicates statistical significance between BEAS-2B and TRPV3OE cells determined using multiple t-tests for each gene and a False Discovery Rate of 5%. Bolded values correspond to a protective effect of TRPV3OE, while italicized values indicate an exacerbation of the response in TRPV3OE cells.

Molecular Pharmacology Fast Forward. Published on September 16, 2020 as DOI: 10.1124/molpharm.120.000047
This article has not been copyedited and formatted. The final version may differ from this version.

Scheme 1: Scheme outlining the integrated ERS response, common stimuli, and common cellular responses. The overall ERS pathway is highlighted in blue, with bold text specifying the biomarkers that were used as indices of ERS in this study. The various ERS-inducing agents that were used are listed in the grey box.

Scheme 2: Proposed mechanism for the regulation of ERS by TRPA1 and TRPV3 in HBECs. WSPM activates TRPA1 and TRPV3 to cause calcium influx and ER calcium release. High intracellular calcium may sensitize/activate TRPV3 on the ER to promote ER calcium release to drive robust ERS responses. Conversely, high levels of intracellular calcium will desensitize TRPA1, leading to a decrease in ER calcium release and ERS, which appears to be driven by TRPV3 activity.

Molecular Pharmacology Fast Forward. Published on September 16, 2020 as DOI: 10.1124/molpharm.120.000047
This article has not been copyedited and formatted. The final version may differ from this version.

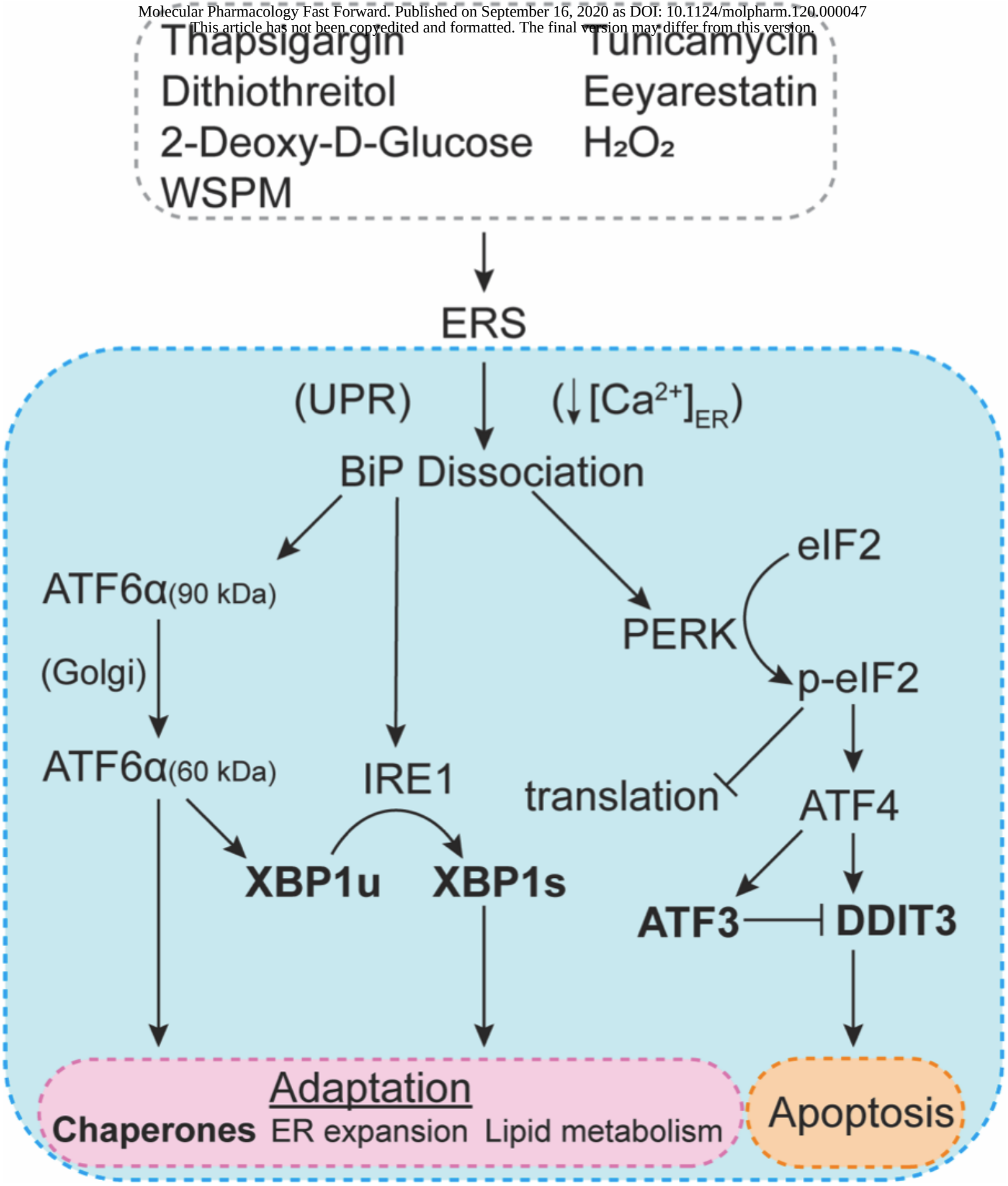

Scheme 1

Molecular Pharmacology Fast Forward. Published on September 16, 2020 as DOI: 10.1124/molpharm.120.000047
This article has not been copyedited and formatted. The final version may differ from this version.

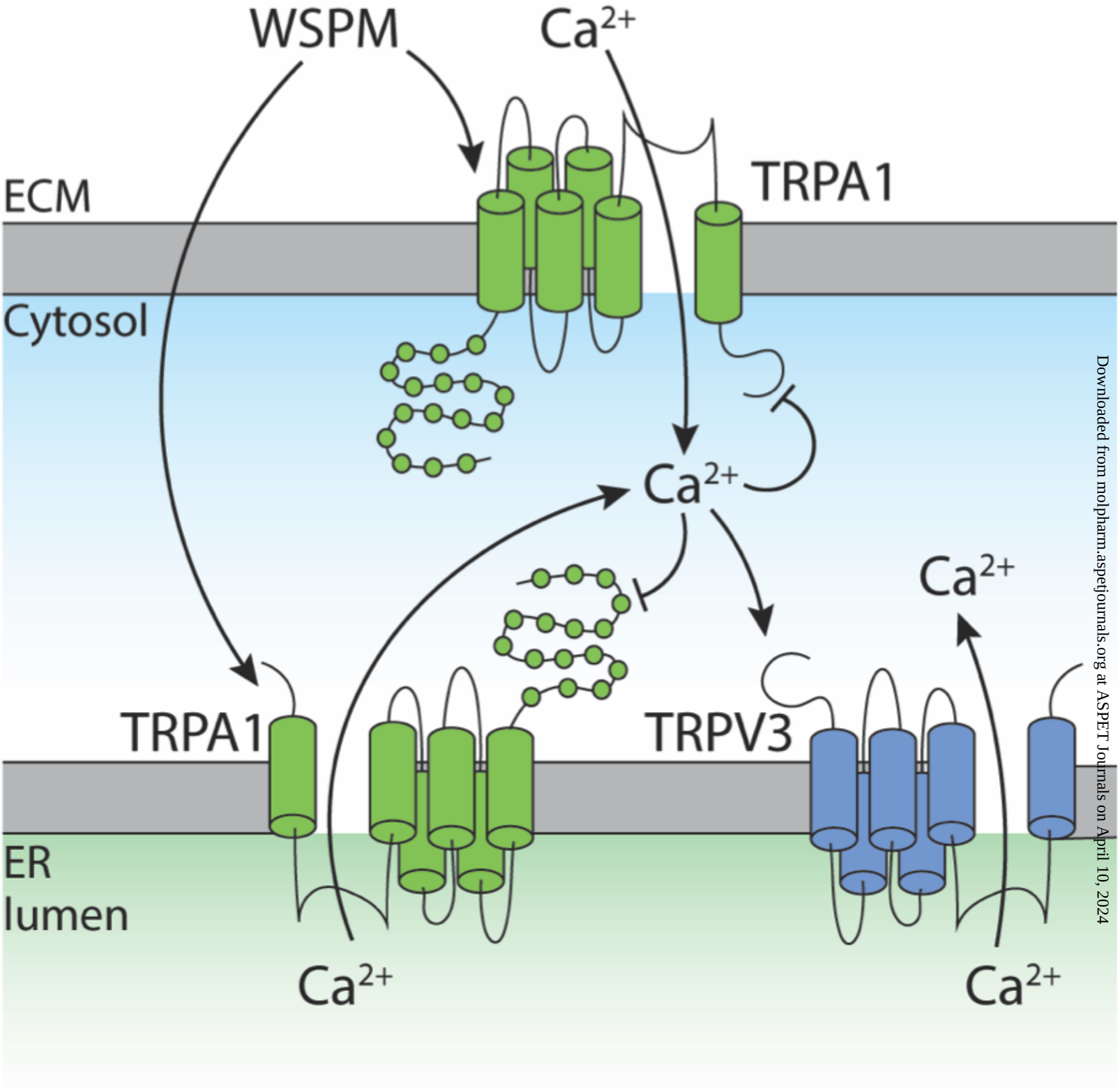

Scheme 2

Molecular Pharmacology Fast Forward. Published on September 16, 2020 as DOI: 10.1124/molpharm.120.000047
This article has not been copyedited and formatted. The final version may differ from this version.

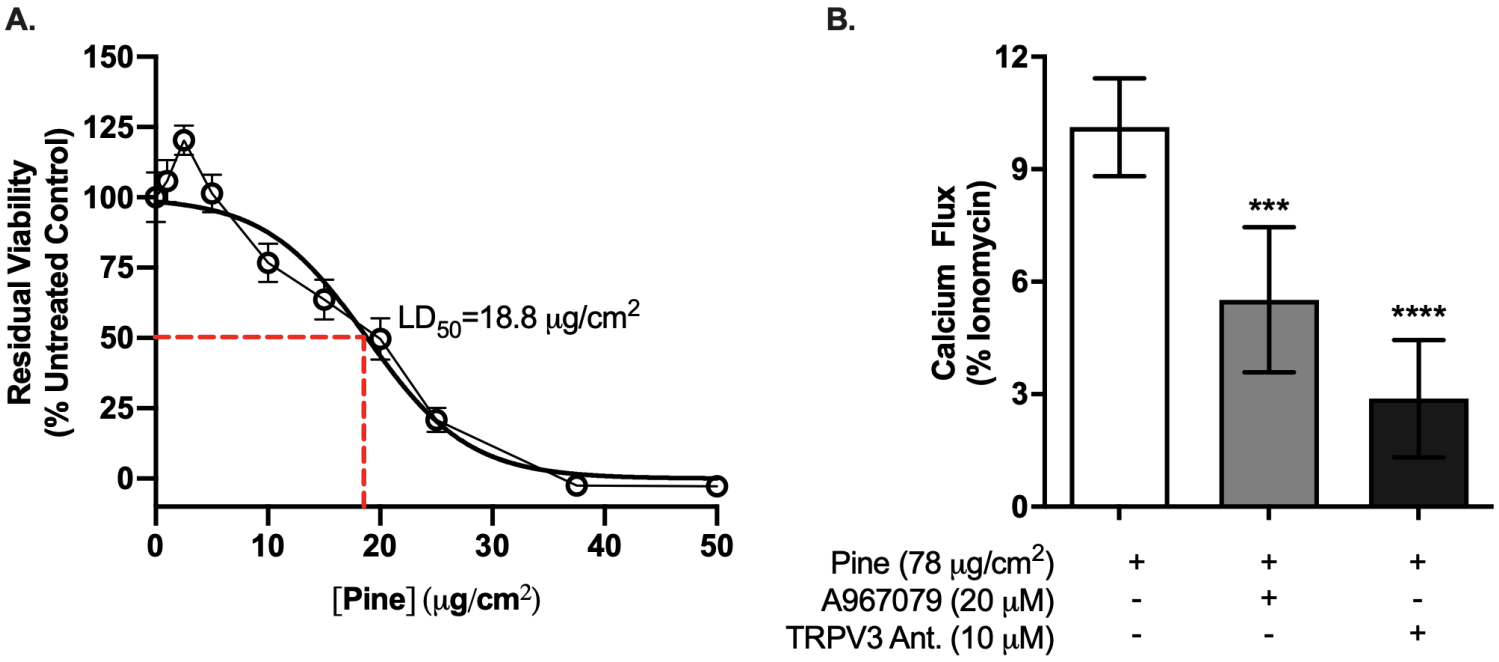

(Figure 1)

A.

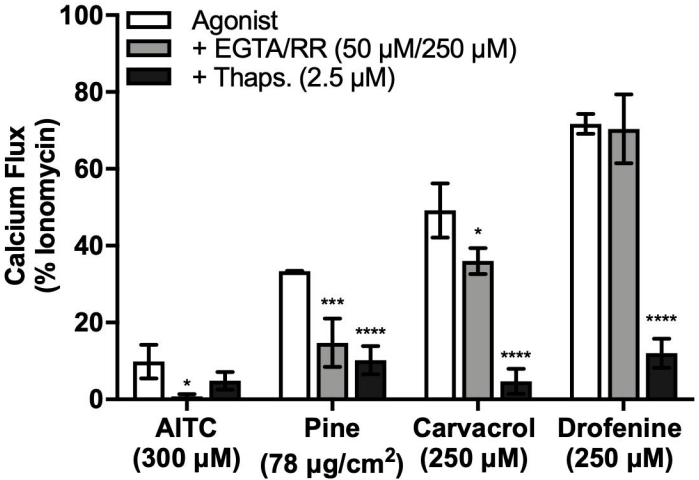
Agonist
+ EGTA/RR (50 µM/250 µM)
+ Thaps. (2.5 µM)
Calcium Flux
(% Ionomycin)
100
80
60
40
20
0
*
***
****
*
****
****
AITC
(300 µM)
Pine
(78 µg/cm2)
Carvacrol
(250 µM)
Drofenine
(250 µM)

B.

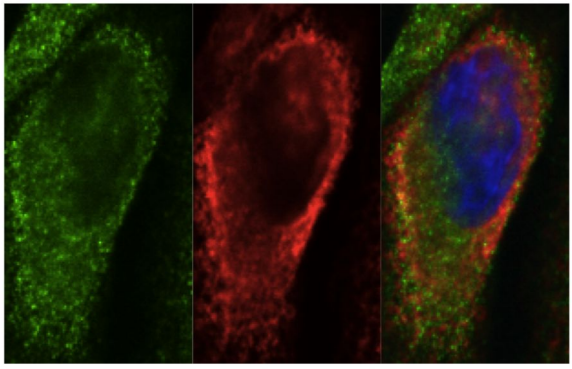

(Figure 2)

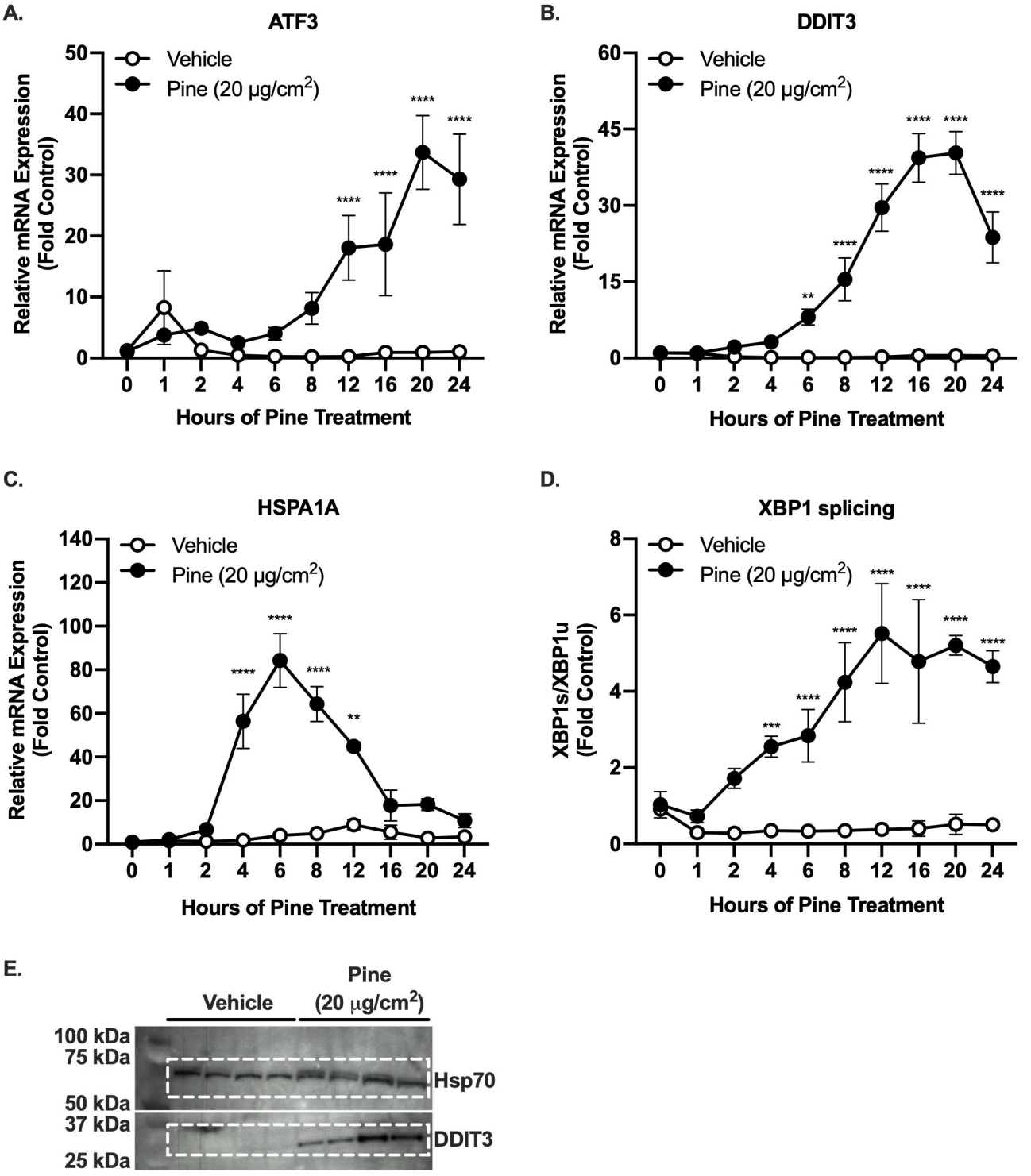
A.
ATF3
Vehicle
Pine (20 µg/cm2)
Relative mRNA Expression (Fold Control)
Hours of Pine Treatment
B.
DDIT3
C.
HSPA1A
D.
XBP1 splicing
XBP1s/XBP1u (Fold Control)
E.
Pine (20 µg/cm2)
100 kDa
75 kDa
50 kDa
37 kDa
25 kDa
Hsp70
DDIT3

(Figure 3)

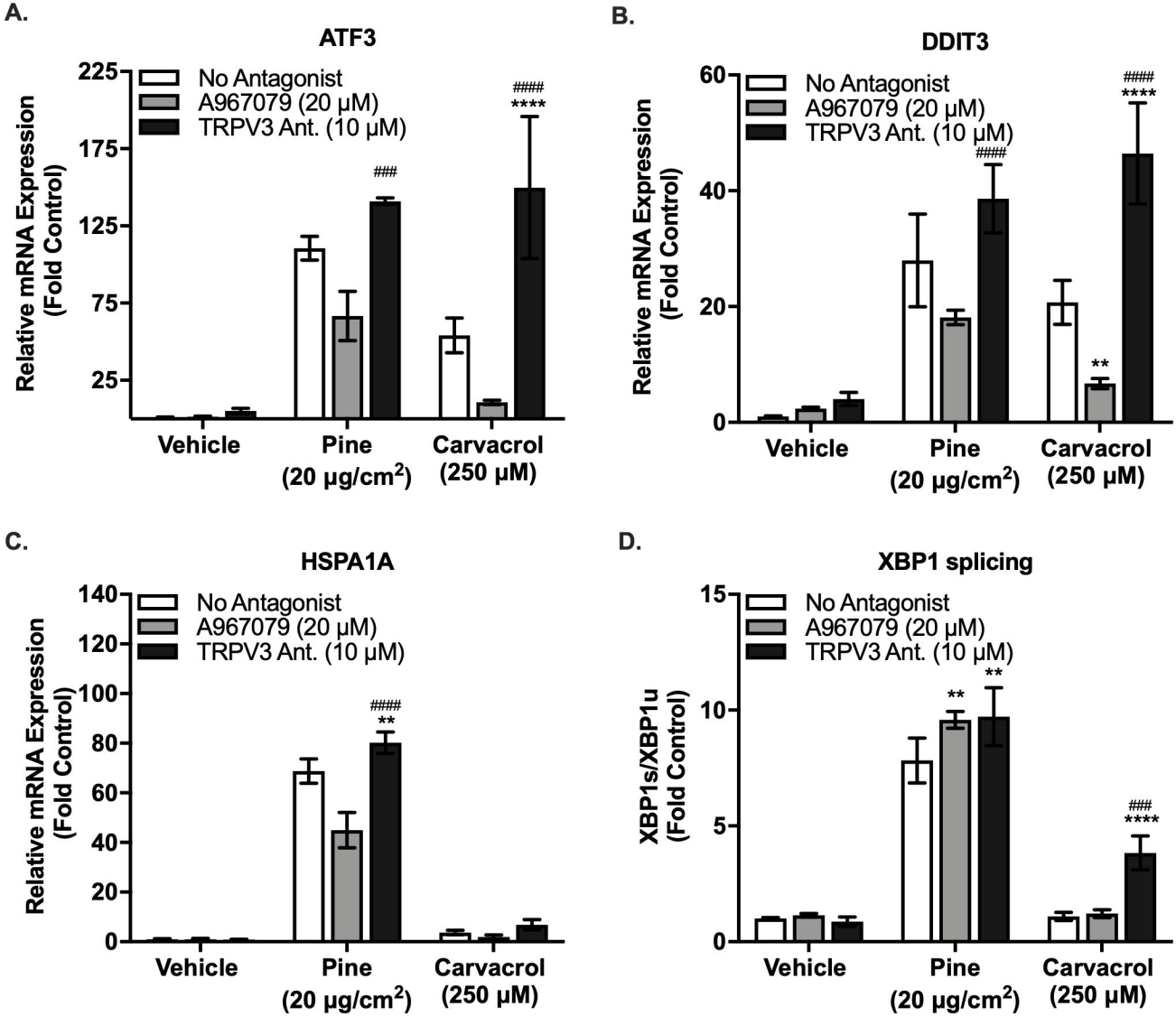
A.
ATF3
No Antagonist
A967079 (20 µM)
TRPV3 Ant. (10 µM)
Relative mRNA Expression (Fold Control)
225
175
125
75
25
###
####
****
Vehicle
Pine (20 µg/cm²)
Carvacrol (250 µM)
B.
DDIT3
No Antagonist
A967079 (20 µM)
TRPV3 Ant. (10 µM)
Relative mRNA Expression (Fold Control)
60
40
20
0
####
**
####
****
Vehicle
Pine (20 µg/cm²)
Carvacrol (250 µM)
C.
HSPA1A
No Antagonist
A967079 (20 µM)
TRPV3 Ant. (10 µM)
Relative mRNA Expression (Fold Control)
140
120
100
80
60
40
20
0
####
**
Vehicle
Pine (20 µg/cm²)
Carvacrol (250 µM)
D.
XBP1 splicing
No Antagonist
A967079 (20 µM)
TRPV3 Ant. (10 µM)
XBP1s/XBP1u (Fold Control)
15
10
5
0
**
**
###
****
Vehicle
Pine (20 µg/cm²)
Carvacrol (250 µM)

(Figure 4)

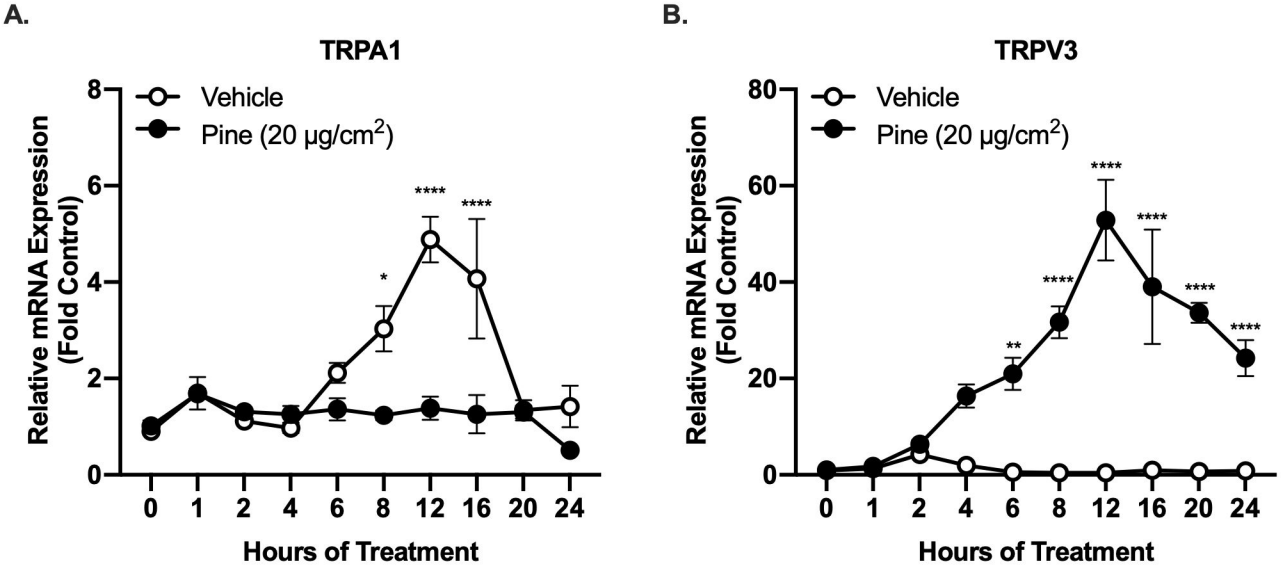
A.
TRPA1
Vehicle
Pine (20 µg/cm2)
Relative mRNA Expression (Fold Control)
0
2
4
6
8
*
****
****
0 1 2 4 6 8 12 16 20 24
Hours of Treatment
B.
TRPV3
Vehicle
Pine (20 µg/cm2)
Relative mRNA Expression (Fold Control)
0
20
40
60
80
**
****
****
****
****
0 1 2 4 6 8 12 16 20 24
Hours of Treatment

(Figure 5)

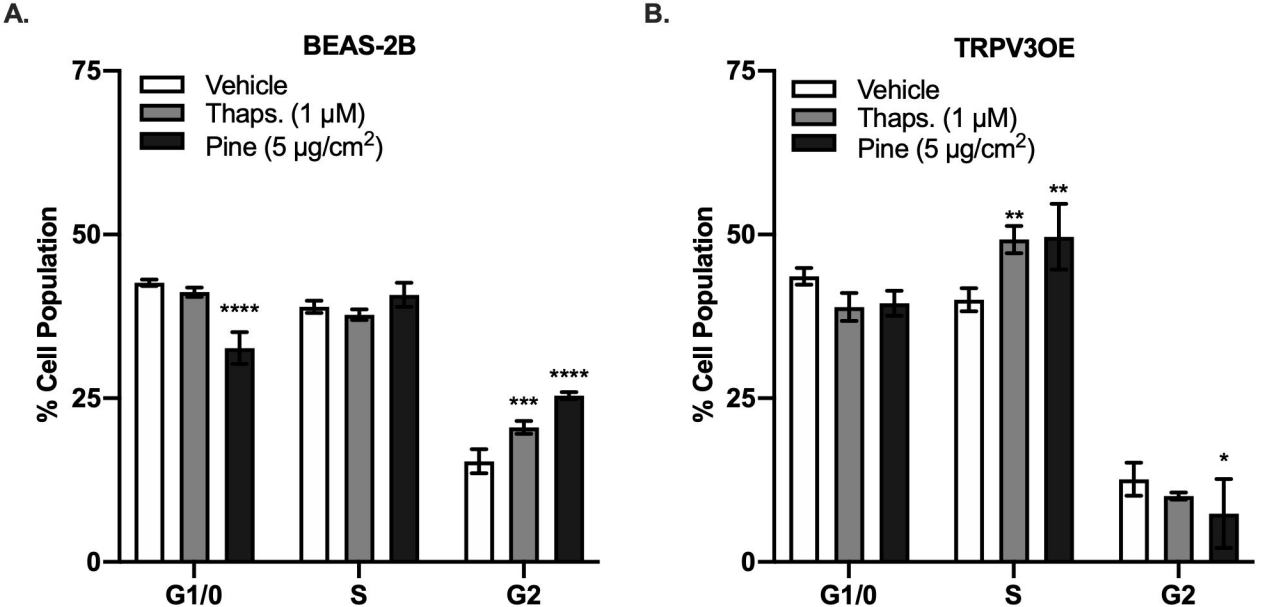
A.
BEAS-2B
Vehicle
Thaps. (1 μM)
Pine (5 μg/cm2)
% Cell Population
75
50
25
0
****
***
****
G1/0
S
G2
B.
TRPV3OE
Vehicle
Thaps. (1 μM)
Pine (5 μg/cm2)
% Cell Population
75
50
25
0
**
**
*
G1/0
S
G2

(Figure 6)

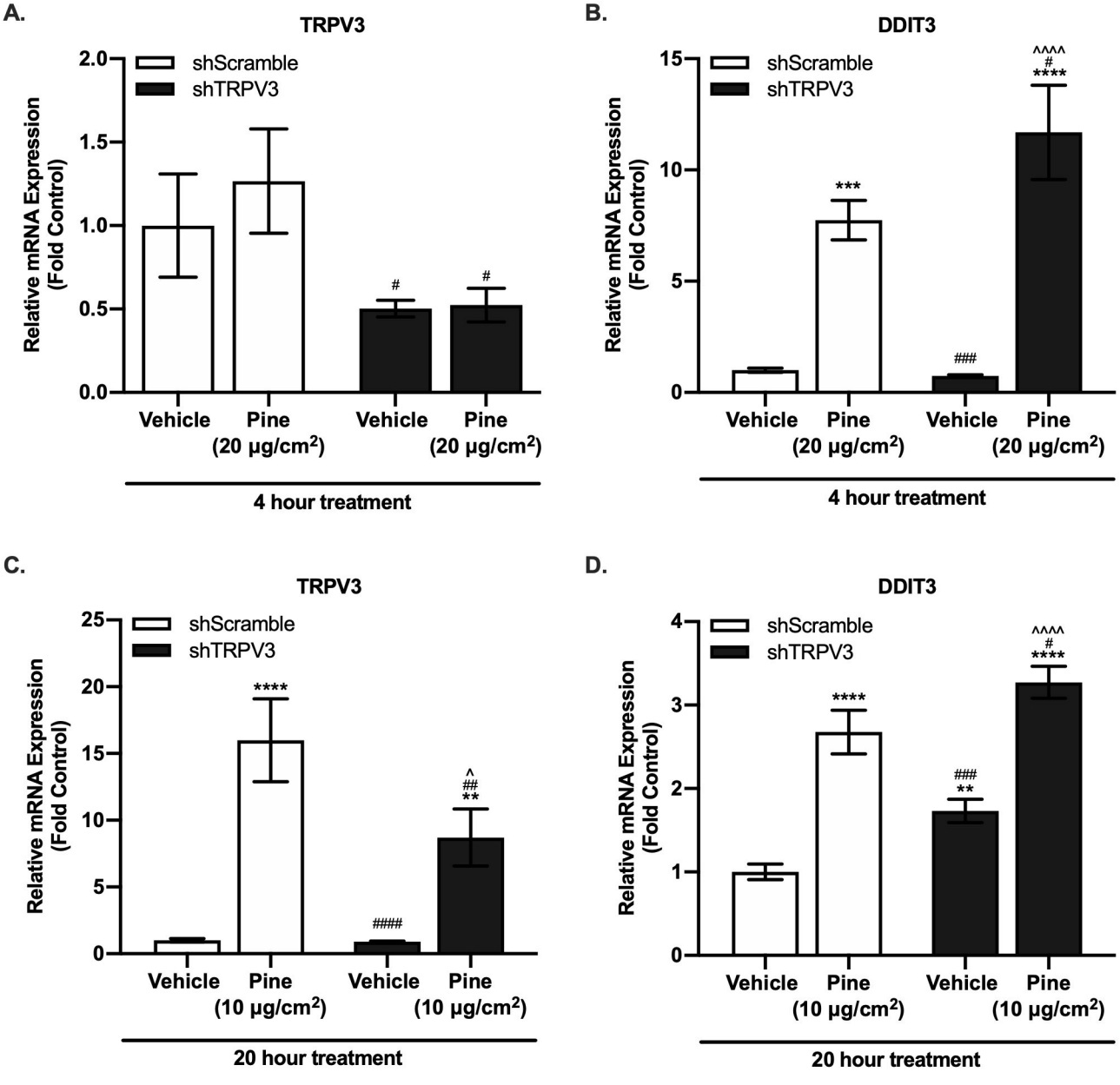
A.
TRPV3
shScramble
shTRPV3
Relative mRNA Expression (Fold Control)
2.0
1.5
1.0
0.5
0.0
#
#
Vehicle
Pine (20 µg/cm²)
Vehicle
Pine (20 µg/cm²)
4 hour treatment
B.
DDIT3
shScramble
shTRPV3
Relative mRNA Expression (Fold Control)
15
10
5
0
***
###
^^^^
#
****
Vehicle
Pine (20 µg/cm²)
Vehicle
Pine (20 µg/cm²)
4 hour treatment
C.
TRPV3
shScramble
shTRPV3
Relative mRNA Expression (Fold Control)
25
20
15
10
5
0
****
####
^
##
**
Vehicle
Pine (10 µg/cm²)
Vehicle
Pine (10 µg/cm²)
20 hour treatment
D.
DDIT3
shScramble
shTRPV3
Relative mRNA Expression (Fold Control)
4
3
2
1
0
****
###
**
^^^^
#
****
Vehicle
Pine (10 µg/cm²)
Vehicle
Pine (10 µg/cm²)
20 hour treatment

(Figure 7)

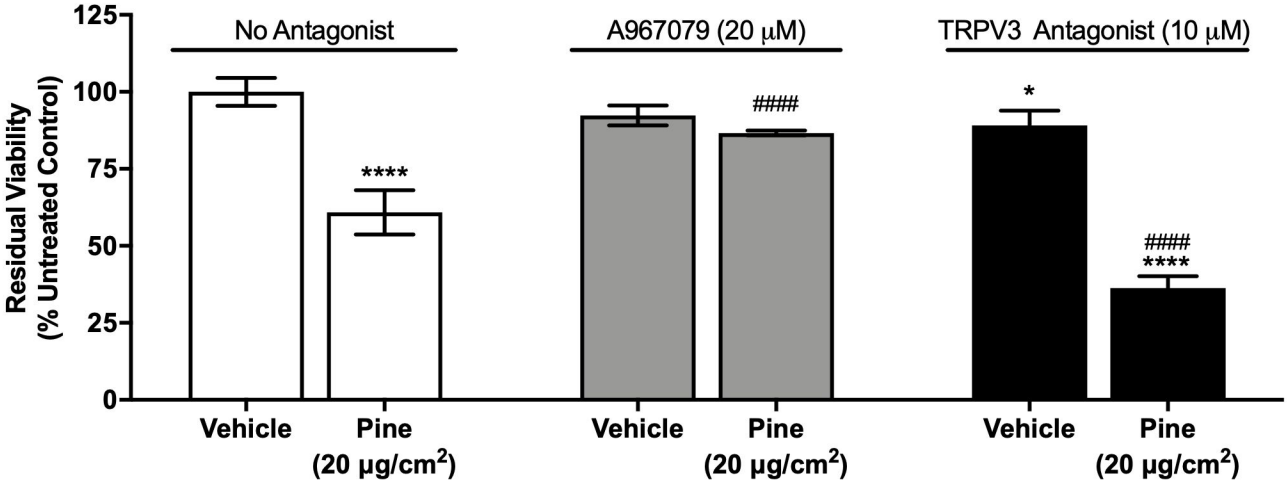
125
100
75
50
25
0
Residual Viability
(% Untreated Control)
No Antagonist
A967079 (20 μM)
TRPV3 Antagonist (10 μM)
****
####
*
####
****
Vehicle
Pine
(20 μg/cm2)
Vehicle
Pine
(20 μg/cm2)
Vehicle
Pine
(20 μg/cm2)

(Figure 8)

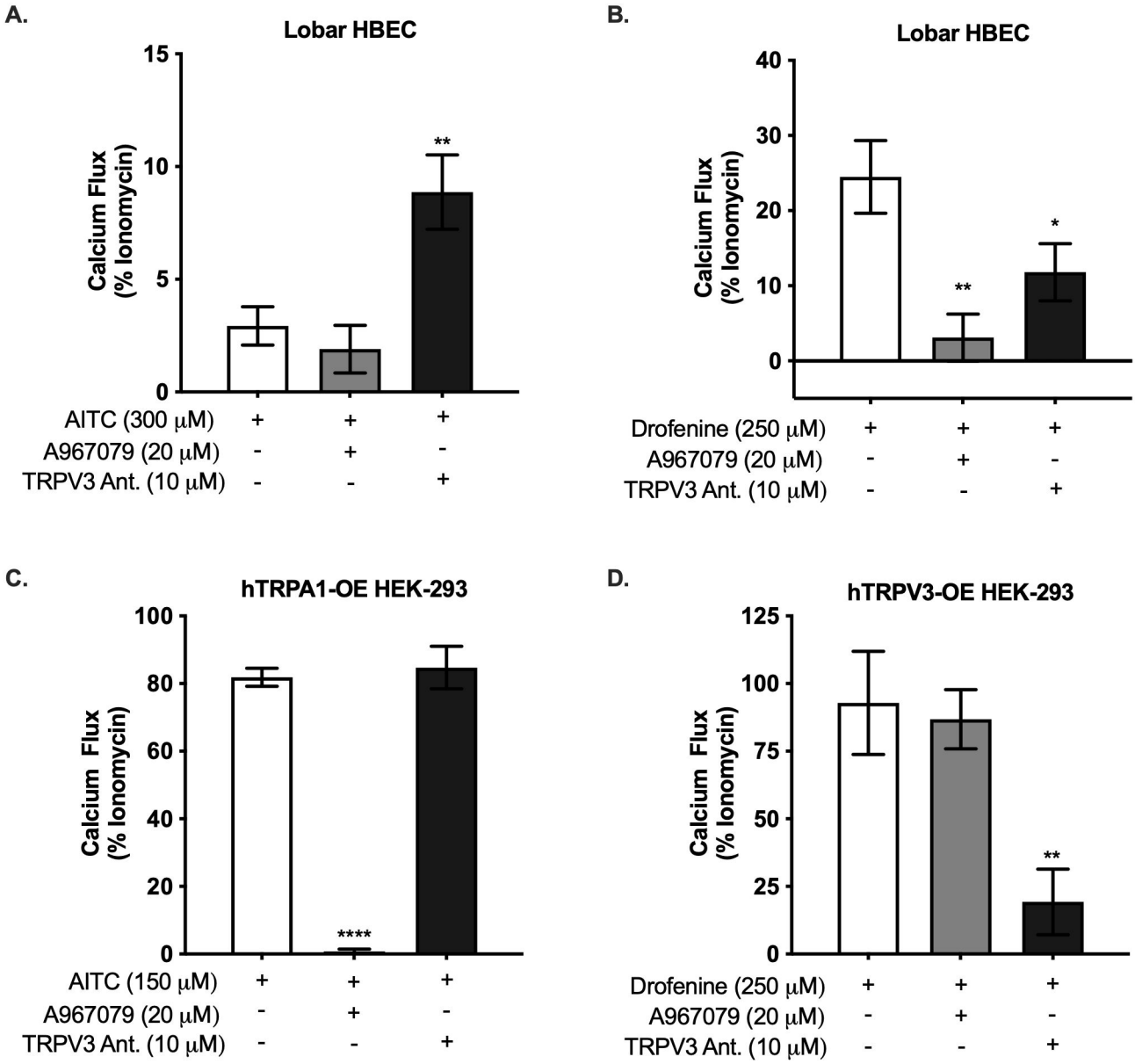
A.
Lobar HBEC
Calcium Flux
(% Ionomycin)
15
10
5
0
**
AITC (300 μM) + + +
A967079 (20 μM) - + -
TRPV3 Ant. (10 μM) - - +
B.
Lobar HBEC
Calcium Flux
(% Ionomycin)
40
30
20
10
0
**
*
Drofenine (250 μM) + + +
A967079 (20 μM) - + -
TRPV3 Ant. (10 μM) - - +
C.
hTRPA1-OE HEK-293
Calcium Flux
(% Ionomycin)
100
80
60
40
20
0
****
AITC (150 μM) + + +
A967079 (20 μM) - + -
TRPV3 Ant. (10 μM) - - +
D.
hTRPV3-OE HEK-293
Calcium Flux
(% Ionomycin)
125
100
75
50
25
0
**
Drofenine (250 μM) + + +
A967079 (20 μM) - + -
TRPV3 Ant. (10 μM) - - +

(Figure 9)